INTERNATIONAL CENTRE FOR THEORETICAL PHYSICS
20 OCT 1982
* LIBRARY *

INTERNATIONAL ATOMIC ENERGY AGENCY
UNITED NATIONS EDUCATIONAL, SCIENTIFIC AND CULTURAL ORGANIZATION

INTERNATIONAL CENTRE FOR THEORETICAL PHYSICS
34100 TRIESTE (ITALY) - P.O.B. 586 - MIRAMARE - STRADA COSTIERA 11 - TELEPHONES: 224281/2/3/4/5/6
CABLE: CENTRATOM - TELEX 460392-I

SMR/98 - 25

AUTUMN COURSE ON GEOMAGNETISM, THE IONOSPHERE
AND MAGNETOSPHERE

(21 September - 12 November 1982)

MAGNETOSPHERE 1

F. MARIANI
Istituto di Fisica
Università degli Studi
Piazzale Aldo Moro 2
00185 Rome
Italy

These are preliminary lecture notes, intended only for distribution to participants.
Missing or extra copies are available from Room 230.

1. Introduction

Until a few decades ago, i.e. before the in situ observations made by artificial satellites and probes, our knowledge on the external environment of the Earth was largely speculative, the best available information being based on relatively simple extrapolation or reasonable hypotheses. With regard to the geomagnetic field the powerful technique of spherical harmonics analysis had already been used to show that the upper atmosphere was a region where electric currents were required to flow to explain the phenomenology of the "external" contributions to the ground observations of some variations of the geomagnetic field (i.e. solar diurnal, S_q; lunar, L). It was also known that in some special occasions, i.e. in association to the geomagnetic storms appropriate current systems were requested to flow either in the upper atmosphere or even at several tens of thousands kms from the Earth to explain the complex observational phenomenology.

The idea that magnetic storms were associated with streams of charged particles impinging on the geomagnetic field and originated on the Sun, most often in coincidence with solar flares, had already been worked out by Chapman and Ferraro in the early thirties. However, the flux of solar particles was considered as an occasional emission propagating through an empty interplanetary medium. Another effect attributed to corpuscolar solar radiation was that of the polar aurora: bombardment of the upper atmosphere at high latitudes by electrons and protons of energies as high as several tens of KeV was shown to be the agent, although essentially nothing was known about the energy source and the acceleration process. The early attempts by Störmer to interpret the polar aurora by means of a stream of ~~individual~~ charged particles directly coming from the Sun, although useful in several respects, did not prove appropriate for the aurora, ~~as we shall see in later sections.~~

An important result by Störmer was the finding of "closed" regions around a dipole magnetic field distribution, closed in the sense that depending upon the actual values of the parameters describing the motion families of particle orbits exist which are not connected to infinity; in other words, not any particle from the Sun can reach the vicinity of the Earth, and particles on closed orbits around the Earth can exist not directly coming from the Sun.

In conclusion, an accepted view of the terrestrial magnetic environment in the fifties was essentially that shown in fig. 1, where the field lines become more and more dipolar as the geocentric distance increased. Charged particles from the Sun were only occasionally present in the interplanetary medium in the shape of large sporadic streams responsible of the geomagnetic storms.

This view has been radically changed since the advent of the satellite age, when a much more complex situation was found (fig. 2).

2. The first pioneeristic experiments.

Apart from several rocket flights giving sporadic informations at altitudes up to a few hundreds kms the first systematic in situ observations of charged particles in the terrestrial environment are those onboard Explorer 1 by means of Geiger counters (launch date 31 january 1958). Fig. 3 shows several counts versus altitude profiles ordered according to the geographical longitudes (left panel) or the magnetic field intensity (right panel). It is quite clear how powerful is the field to organize the data; it is also evident a 3 orders of magnitude increase of the counting rates at a critical altitudes where the field becomes less than about 0.22 gauss (i.e. altitudes between 400 and 1400 kms on the ground, depending upon the longitude). It is worth noticing that before Explorer I, another man-made vehicle, Sputnik II, launched on Nov. 3, 1957, has Geiger counters onboard; however, due to the highly inclined orbit with perigee ~~in the north~~ at high (latitude) northern, when it could be monitored in URSS, it was constantly underneath the radiation belt later discovered by Explorer I. The first exploration at higher distances is due to the space probes Pioneer III and IV which showed two relative maxima of the counting rates, one at about 3000 kms on Earth, the second one at or above 25000 kms. In the few years following this initial phase, a very intense phase of pioneeristic study has been conducted by several s/c. We only mention here the other fundamental in situ discovery in the early sixties of the corpuscolar solar radiation, the solar wind, onboard Lunik II and III in a rather qualitative way and shortly later onboard Explorer X (or IMP-1) and Mariner 2. Fig. 4 shows some basic information on the plasma and magnetic field detected onboard Explorer X.

3. A summary of basic instrumentation.

In this section we shall shortly describe some basic instruments used to detect either ~~magnetic~~ fields or particles. As regards particles our attention will be limited essentially to distinguish low energies of the order of a few to a ~~few~~ tens keV ~~[illegible]~~; detectors for higher energies up to hundreds MeV as observed in the innermost region of the radiation belts are somewhat more conventional so we shall ~~only say a few words about them~~ not consider them.

3.1. Magnetic field detectors for space research.

3.1.1. Instruments for d.c. measurements.

Measurements of d.c. magnetic fields in the magnetosphere have been performed by different techniques. The most used vector instrument, also capable to follow variations up to several Hz, is the saturation or flux-gate magnetometer, based on the non linear response of monoaxial magnetically saturable core sensors. Each sensor is excited at a frequency f, typically several KHz, to saturation, i.e. to the region of strong non linearity of the B-H hyste resis curve. By means of two similar parallel linear elements excited in opposition of phase and of a secondary coil surrounding both elements it is possible to get an induced e.m.f. at frequency 2f proportional to the ambient field component along the sensor axis. A combination of three orthogonal identical sensors allows determination of the full magnetic vector. Big improvement on the sensor has been ~~made~~ possible using toroidal or ring cores. Although, in principle, considerable noise may be expected it is now possible by using ~~toroidal or ring~~ such cores to get extremely good performances, in particular sensitivity and stability ~~such~~ so to make the flux gate magnetometer an ideal instrument. The real problem of a magnetic measurement is actually not the instrument, but, rather, the magnetic contamination produced onboard any space vehicle by the mechanical structure (remnant magnetism) and/or by the electric and magnetic circuitry. This is expecially the case when absolute fields as low as a few gammas or even fractions of gammas are to be measured. On spinning spacecraft the two field components perpendicular to the spin axis can be easily corrected for any <u>constant</u> spurious field due to the fact that this rotates with the spacecraft. The third, spin-axis, component however must be corrected by using a physical inversion of the sensor (for example by a flipper mechanism) or by a different concept using a dual magnetometer technique, i.e. by adding another magnetometer closer to the spacecraft body. Comparing the measurements by the

two instruments, assuming some simple description of the spurious field (for example as dipole field) it is thus possible to extract the absolute spin field component. As an example some details on the fluxgate magnetometer to be used in the frame of the multispacecraft mission OPEN are given in fig.5

Another instrument for vector field measurement is the helium vector magnetometer, based on quantum properties of the electrons in the helium atom. Absolute field strengths (and, with some experimental tricks, components) can also be measured by means of the alkali-vapour and the nuclear precession absolute magnetometers (the latter, however, is more appropriate for higher fields, as those found close to or on Earth). A description of the above instruments, which is beyond the purpose of this review essentially limited to magnetosphere, can be found in several good review papers on the subject.

3.1.2. <u>Instruments for A.C. measurements.</u>

The instrument described in the previous section does not have sufficient sensitivity at frequencies above a few Hz. Above 10 Hz an induction (or search-coil) device has increasingly superior performances. The basic concept is that of using as magnetic antennas three orthogonal high permeability μ-metal cores wound with thousands turns of wire. The induced e.m.f. produced by variations of any magnetic field component B_i measured is proportional to the time derivative $\frac{dB_i}{dt}$ so that the sensitivity of the instrument linearly increases with increasing fluctuation frequency, the upper limit actually being set by the natural resonances of the coil + core system. The full frequency band is usually divided into several channels by appropriate filters so to make possible spectral analysis of the signal. As an example, the search coil magnetometer flown on ISEE 1 has a sensitivity of 35 μ volt/(γ $\cdot$ Hz), ~~with~~ an upper cut-off frequency at 10 KHz ~~with~~ and 14 channels covering the range from 5.6 to 10^4 Hz. ~~with the magnetic field spectral noise level shown in fig.6~~

3.2. Electric field instruments.

The importance of electric field measurements has been recognized for some time, but only recently has gained sufficient attention, in particular due to the discovery that substantial magnetic field aligned electric fields exist in regions of thousands of kms in altitude. The physical implications of such fields are far reaching: for example the frozen-in field condition can be violated and the mapping of the electric field in the outer magnetosphere along the magnetic field lines is no longer allowed.

3.2.1. The basic concept of a quasi-static or low frequency electric field measurement is that of using the potential difference existing at the two ends of long sensors. These have to be long

enough to be well out of the perturbed plasma sheath around the spacecraft. The two tips of the sensor, symmetrical with respect to the main body of spacecraft, may be identical spheres or linear elements. The potential difference is given by $\Delta V = (\underline{E} + \underline{v} \times \underline{B}) \cdot \underline{d}$ where $\underline{d}$ is the distance of the two tips, $\underline{v}$ the translation velocity of the satellite relative to the inertial system of plasma, $\underline{B}$ the magnetic field and $\underline{E}$ the electric field. Determination of $\underline{E}$ requires very precise knowledge of $\underline{v}$ and $\underline{B}$ (it should be pointed out that $\underline{v} \times \underline{B}$ is of the order of tenths of volt/m, while $\underline{E}$ is only of the order of a few m Volt/m; also contact potentials play a large perturbing role to be taken care of). As examples of electric instruments we show in fig. 6 the configuration of a dual-probe antenna flown on ISEE-1 (~~left~~ upper panel) and a diagram (~~right~~ lower panel) showing the electric field component (spin modulated) in the ecliptic plane (by definition proportional to the magnetic field component perpendicular to ecliptic, also shown in the panel), as measured on ISEE by a spherical dual probe detector.

3.3. Particle instruments

3.3.1. Detection of particles is achieved by different methods, depending upon what one is actually interested in : energy or angular spectra, mass and charge composition, energy range. Generally speaking, particle densities in the interplanetary medium and in the magnetosphere are very small, from a few tenths to a few hundred per cm^3 and the smallest typical length, the Debye length, is much larger than the size of the instruments used to detect the particles. So the "macroscopic" properties, like density n, bulk velocity $\underline{V}$, pressure P, heat flux q, and so on are to be derived by appropriate treatment of the distribution function $f(\underline{v})$ of the velocity. For example the above quantities (for the case of a single component (gas)) are obtained by means of

$$(3.1)\left\{\begin{aligned} n &= \int f(\underline{v})\, d^3\underline{v} \\ \underline{V} &= \frac{1}{n}\int \underline{v}\, f(\underline{v})\, d^3\underline{v} \\ P &= m\int f(\underline{v})\,(\underline{v}-\underline{V})^2\, d^3\underline{v} \\ q &= \frac{1}{2} m \int f(\underline{v})\,(\underline{v}-\underline{V})\,|\underline{v}-\underline{V}|^2\, d^3\underline{v} \end{aligned}\right.$$

The "temperature" T is defined by T = p/nm; it is a tensor since p is also a tensor. This temperature is thus a measurement of the spectral width of $f(\underline{v})$. The parameters experimentally measured are counting rates C, current intensity I and flux F. Taking again a mono-component particle gas they are defined by

$$(3.2)\quad C(\underline{u}) = S\int v_n\, f(\underline{v})\, G(\underline{u},\underline{v})\, d^3\underline{v}$$

where $\underline{u}(\vartheta,\varphi)$ is the velocity relative to the detector, in a direction ϑ and φ with respect to the normal n to the detector surface, $G(u,v)$ is the transparency of the detector

$$(3.3)\left\{\begin{aligned} I(\underline{u}) &= e\, C(\underline{u}) \\ F(\underline{u}) &= C(\underline{u})/S \end{aligned}\right.$$

where e is the particle charge and S the area of the detector. Equation (3.2) is an integral equation in $f(\underline{v})$ which in principle can be derived and afterwards used to compute the macroscopic parameters. It is quite clear that determination of $f(\underline{v})$ is not that simple, so usually a maxwellian or a bimaxwellian distribution is assumed whose free parameters are best fitted to the experimental observations.

3.3.2. The basic instruments for detection of solar wind particles are <u>Faraday cups</u> and <u>electrostatic analyzers</u>, whose operation concepts are shortly illustrated in fig. 7. Particles impinging on the aperture of a Faraday cup go through several grids at appropriate potentials: G1 and G3 act as screens to avoid external effects from the internal electrical fields and respectively to screen the collector C; G4 rejects toward C any secondary electron; finally a step modulated variable potential square wave ΔV modulates the current reaching the collector C which gives a measurement of the energy window content $e\Delta V$.
In the case of electrostatic analyzers, two concentric portions of spherical surfaces are essentially charged by a potential difference ΔV: particles going through the aperture are deflected, only those in a certain energy range ΔE being capable to reach the collector; the sensitivity and the directional response of this instrument is greatly improved by means of channel electron

multipliers appropriately located. Fig. 8 shows a sketch of the quadrispherical analyzer used onboard ISEE-1 and 2, capable to determine the directional intensities of positive ions and electrons over all but 2% of the full 4π solid angle, in an energy range from 1eV to 45 keV per unit charge.

At higher energies particle properties can be obtained by means of somewhat more complex techniques, depending upon the energy range. Also detectors ~~can be~~ become different, although somewhat more conventional. We feel this ~~also~~ is beyond the limits of our review, so reference ~~is~~ should be made to appropriate review papers and specialized literature.

4. Motion of charged particles in a magnetic field.

The equation of the motion of a particle of charge e, mass m, in a field $\underline{B}$ under the action of an electric field $\underline{E}$ and a non electromagnetic force F can be written as follows (using rationalized MKSQ units):

$$(4.1) \quad \frac{d\underline{p}}{dt} = e\left(\underline{E} + \underline{v} \times \underline{B}\right) + \underline{F}$$

where $\underline{p}$ is the momentum $m\underline{v}$. A special case of (4.1) where $\underline{F} = \underline{E} = 0$ and $\underline{B}$ is ~~the~~ a dipole field is the equation originally treated by Störmer. Although simple in principle, the Störmer's case is already complicate; only a first integral is found but no general analytical solution can be written. (see section 4.4). So, only under simplyfying assumptions one can find reasonably simple approximate solutions of (4.1). In particular, we shall show existence of three typical periodicities, valid under physically different restrictions.

4.1. If the field $\underline{B}$ is slowly variable versus time and space, the motion of a particle can be decomposed in a linear motion at a velocity $\underline{v}_\parallel$ along the field line and a nearly-circular drift motion on a plane perpendicular to it and moving at the velocity $v_\parallel$. The center of the motion on this plane is called guiding center. The physical conditions for this to be true are that

$$(4.2) \quad \frac{1}{B}\frac{\partial B}{\partial t} \ll \frac{1}{T_c} = \frac{eB}{2\pi m} \quad \text{and} \quad \frac{1}{B}\frac{\partial B}{\partial \underline{z}} \ll \frac{1}{R_c} = \frac{eB}{mv}$$

where T_c and R_c are the cyclotron (or Larmor) period and radius, respectively. In general, the guiding center may have a velocity $\underline{V}_D$ normal to $\underline{B}$, describing a drift across the field lines. The velocity $\underline{v}'$ of the particle and the electric and magnetic fields $\underline{E}'$, $\underline{B}'$, as seen on the moving plane are thus respectively defined by:

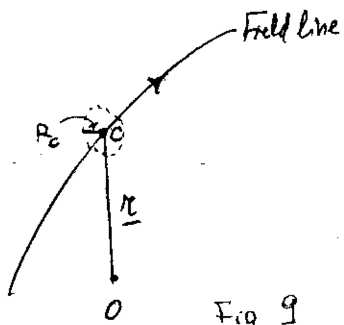

Fig 9

$$(4.3) \quad \begin{aligned} v'_\parallel &= 0 & \underline{B}' &= \underline{B} \\ \underline{v}'_\perp &= \underline{v}_\perp - \underline{V}_D & \underline{E}' &= \underline{E} + \underline{V}_D \times \underline{B} \end{aligned}$$

Several special cases can be specified, as shown below.

4.1.1. The field $\underline{B}$ is static and uniform, and $\underline{F} = 0$. It is obvious that the parallel component of $\underline{p}$ (and $\underline{v}$) is constant, due to the fact that the acting force (Lorentz force) is by definition normal to B. So $v_{\parallel}$ = const (uniform rectilinear motion along the field). Also $v_{\perp}$ (and $p_{\perp}$) must thus be constant in value, which means the motion projected on a plane perpendicular to the field is exactly circular and uniform. Positive and negative particles rotate at the same angular velocity in opposite directions. As an example, with B=0.5 G a proton has a cyclotron period $T_c \approx 0.13\ \mu sec$ and a giroradius $R_c = \frac{v_\perp T_c}{2\pi} \approx 2 \cdot 10^{-8}\, v_\perp$. With $v_\perp = 10^6$ m/sec (i.e. a proton energy of 5 KeV) R_c is only 2 cm! So, for a time constant geomagnetic field the second of the two conditions (4.2) is generally satisfied except for particles with very high energy (as for example cosmic rays).

4.1.2. The field $\underline{B}$ is static and uniform, but $\underline{F}$ is not zero, although static and uniform.

In this case, equation (4.1) can be written as

$$(4.4)\qquad \frac{dp_\parallel}{dt} = \underline{F}_\parallel$$

$$\frac{dp_\perp}{dt} = \underline{F}_\perp + e\,\underline{v}_\perp \times \underline{B}$$

which indicates that the motion parallel to $\underline{B}$ is only governed by the component $\underline{F}_{\parallel}$ (the particular case $\underline{F}_{\parallel} = 0$ implies that $\underline{v}_{\parallel}$=const). On the movable plane the guiding center has a rectilinear motion, i.e. there is balance between the induced electric field and the force $\underline{F}_\perp$ which requires $e\,\underline{V}_F \times \underline{B} + \underline{F}_\perp = 0$

From here we easily get the drift velocity

$$(4.5)\qquad \underline{V}_F = \frac{\underline{F}_\perp \times \underline{B}}{e B^2} = \frac{\underline{F} \times \underline{B}}{e B^2}$$

which implies opposite orientations for negative and positive charges. Equation (4.5) is valid under the condition that $F_\perp / eB \ll c$ here c is the velocity of the light. This is not a stringent condition. A special case of (4.5) occurs when $\underline{F}$ is an electric force $e\underline{E}$: this case implies cancellation of the charge e so that either positive or negative particles drift in the same direction.

4.1.3. The magnetic field B is not uniform and F = 0.

In this case we can in general write the field component B_i as

$$(4.6)\qquad B_i = B_{oi} + \sum_J \alpha_{iJ}\,\Delta x_J \qquad (i=1,2,3),\ (J=1,2,3)$$

where B_{oi} is the component i of the field in the origin and B_i the same component in another point displaced of Δx_i(i=1,2,3) by the origin and $\alpha_{iJ} = \frac{\partial B_i}{\partial x_J}$.

The equation (4.1) can be solved by iteration. Let us put, as first approximation $\alpha_{iJ} = 0$ i.e. $B_i = B_{oi}$, which is the case already considered in the section 4.1.1. The velocity of motion is known and satisfies the equation $m\ddot{\underline{x}}_o = e\,\dot{\underline{x}}_o \times \underline{B}_o$.

We then proceed with the second approximation

$$(4.7)\quad \begin{cases} \Delta x_i = \dot{x}_{oi}\,\Delta t \\ \dot{x}_i = \dot{x}_{oi} + V_i \end{cases}$$

where $\underline{V}\,(\ll \dot{\underline{x}}_o)$ is the perturbation added ~~on~~ to the velocity $\dot{\underline{x}}_o$. As a consequence the velocity $\underline{V}$ must satisfy the equation

$$(4.8)\quad \dot{\underline{V}} = \frac{e}{m}\left[\underline{V}\times\underline{B}_o + \underline{f}(t)\right] \qquad \text{with } \underline{f}(t) = \dot{\underline{x}}_o \times \sum_j \alpha_{ij}\,\Delta x_j$$

and hence

$$(4.9)\quad \ddot{\underline{V}} = \frac{e}{m}\left[\dot{\underline{V}}\times\underline{B}_o + \frac{d\underline{f}}{dt}\right]$$

Substitution of $\dot{\underline{V}}$ from (4.8) in (4.9), with $\underline{\omega} = \dfrac{e\underline{B}_o}{m}$ leads to

$$(4.10)\quad \ddot{\underline{V}} + \underline{\omega}\times\left[\underline{f} - \underline{\omega}\times\underline{V}\right] = \frac{d\underline{f}}{dt}$$

from which, we get

$$(4.11)\quad \ddot{\underline{V}} + \omega^2\underline{V} = \dot{\underline{f}} - \underline{\omega}\times\underline{f} + (\underline{\omega}\cdot\underline{V})\,\underline{\omega}$$

and finally, ~~after~~ using (4.8) and noticing that $\underline{\omega}\cdot(\underline{\omega}\times\underline{V}) \equiv 0$,

$$(4.12)\quad \ddot{\underline{V}} + \omega^2\underline{V} = \dot{\underline{f}} - \underline{\omega}\times\underline{f} + \underline{\omega}\int_0^t \dot{\underline{\omega}}\cdot\underline{f}\,dt\ .$$

At this point, use of the first approximation velocity $\dot{\underline{x}}_o$ in the expression of $\underline{f}$, leads to the following expressions of velocity components V_i (i=1,2,3)

$$(4.13)\quad \begin{cases} V_1 = -\dfrac{e}{m\omega^2}\left(\frac{1}{2}\alpha_{32}v_\perp^2 + \alpha_{23}v_\parallel^2 - \omega\,\alpha_{13}v_\parallel^2 t\right) \\ V_2 = \dfrac{e}{m\omega^2}\left(\frac{1}{2}\alpha_{31}v_\perp^2 + \alpha_{13}v_\parallel^2 + \omega\,\alpha_{23}v_\parallel^2 t\right) \\ V_3 = -\dfrac{e}{m\omega}\,\frac{1}{2}\alpha_{33}v_\perp^2 t \end{cases}$$

Simple inspection of the terms in (4.13) shows immediately that V is made by three motions with respective velocities $\underline{v}_l$, $\underline{v}_i$, $\underline{v}_r$ defined by the vectors

$$(4.14)\quad \underline{v}_l = \frac{1}{B_o}\left[\alpha_{13}v_\parallel^2 t\,,\ \alpha_{23}v_\parallel^2 t\,,\ -\frac{1}{2}\alpha_{33}v_\perp^2 t\right]$$

$$(4.15)\quad \underline{v}_i = \frac{v_\perp^2}{2\omega B_o}\left[-\alpha_{32}\,,\ \alpha_{31}\,,\ 0\right] = \frac{v_\perp^2}{2\omega B_o}\,\underline{u}\times\underline{\nabla}B \qquad \underline{u} = \underline{B}_o/B_o$$

$$(4.16)\quad \underline{v}_r = \frac{v_\parallel^2}{\omega B_o}\left[-\alpha_{23}\,,\ \alpha_{13}\,,\ 0\right] = \frac{v_\parallel^2}{\omega B_o}\,\underline{B}\times\frac{\partial\underline{u}}{\partial s} = \frac{v_\parallel^2}{\omega B_o}\,\underline{B}\times\frac{\underline{n}}{R}$$

where R is the curvature radius of the field line and $\underline{n}$ the principal normal to the field line (or binormal).

In our first order approximation it is easily recognized that the vector $\underline{v}_\parallel + \underline{v}_l$ is parallel to the vector $\underline{B}$, so that it represents the velocity along the field line; the velocity $\underline{v}_i$ represents the so-called inhomogeneity drift velocity, normal to $\underline{B}$ and its gradient ;

finally, the velocity $\underline{v}_r$ represents the curvature drift velocity normal to either $\underline{B}$ or the ~~principal~~ binormal $\underline{n}$. ~~to the field line, or~~

~~oriented along the so called binormal to the field line.~~

An obvious condition attached to the inhomogeneity drift (4.15) is that the $\nabla_\perp B$ be small over a cyclotron orbit, i.e. that $\nabla_\perp B \ll B/\rho_c$ or $R = B/\nabla_\perp B \gg \rho_c$ where ρ_c is the cyclotron radius.

It is to be noticed that $\underline{v}_i$ and $\underline{v}_r$ both point in the same direction, since $\underline{n}$ has the same direction of $\nabla_\perp$ B.

4.1.4. Drifts associated with time dependence.

Drifts of such a kind arise because of the fact that when the drift velocities, as given in previous sections, are time dependent (for example because of a time dependent electric field) an additional acceleration $m\dot{\underline{V}}$ arise to modify the guiding centre velocity. In this case by means of equation (4.5) the additional drift velocity can be expressed by

$$(4.17) \quad \underline{V} = -\frac{\dot{\underline{V}}}{\omega B} \times \underline{B}$$

which however requires the condition $T_c \dot{V}/V \ll 1$, where T_c is the period of a cyclotron rotation. Equation (4.5) also implies (in the case of a variable electric field $\underline{E}$) that $\dot{\underline{V}} = \frac{\dot{\underline{E}} \times \underline{B}}{B^2}$ so that (4.17) leads to the expression of the so called polarization drift

$$(4.18) \quad \underline{V}_p = \frac{\dot{\underline{E}}}{\omega B}$$

4.2. The adiabatic invariants

There are some physical entities which under appropriate conditions have the property of being almost constant to deserve the name of adiabatic invariants.

4.2.1. The first adiabatic invariant.

This invariant is also indicated as magnetic moment invariant. According to equation (4.14) the increment of the longitudinal velocity in the time interval Δt is given by

$$(4.19) \quad \Delta \dot{v}_{\parallel} = \dot{v}_{\parallel} \Delta t = -\frac{\alpha_{33} v_\perp^2}{2B_0} \Delta t = -\frac{v_\perp^2}{2B} \frac{\partial B_3}{\partial x_3} \Delta t = -\frac{v_\perp^2}{2B} \left(\frac{\partial B}{\partial \ell}\right)_0 \Delta t$$

where ℓ is the curvilinear coordinate along the field line.

From (4.19) we can immediately derive the equation of the motion of the dipole equivalent to the particle along the line of force

$$(4.20) \quad m \dot{v}_{\parallel} = -\mu \frac{\partial B}{\partial \ell} \qquad \text{where } \mu = -\frac{1}{2} \frac{m v_\perp^2}{B}$$

This equation can be easily transformed into

$$(4.21) \quad \frac{d}{dt}\left(\frac{1}{2} m v_{\parallel}^2\right) = -\mu \frac{dB}{dt}$$

or, because of the constancy of the kinetic energy $\frac{1}{2} m v^2$ implying $\frac{d}{dt}\left(\frac{1}{2} m v_{\parallel}^2\right) = -\frac{d}{dt}\left(\frac{1}{2} m v_\perp^2\right)$ into

$$(4.22) \quad \frac{d}{dt}(\mu B) - \mu \frac{dB}{dt} = 0$$

from which it follows that the magnetic moment must remain sensibly constant during the motion. In other words, the magnetic moment μ is an invariant, under the restriction that the magnetic field B is only slightly variable over a Larmor orbit. If the angle α of the velocity vetcor $\underline{v}$ to the field $\underline{B}$ is introduced, it is immediately recognized that the condition $\frac{\sin^2\alpha}{B} = \frac{1}{B_m} = \longrightarrow$ const must hold, B_m being the field strength at the point where $\alpha = \pm 90°$. The field B_m represents the maximum field achievable to the particle. The two points corresponding to the limit values are called mirror points, ~~in the sense~~ to mean that at these points particles are reflected as a consequence of the sign change in the longitudinal velocity.

4.2.2. The second adiabatic invariant.

The periodicity of motion between the mirror points implies a trapping of the particle which, unless external forces are taken into account, will undefinitely continue its bounce motion between conjugated points with a parallel velocity $v_{\parallel}(\ell) = v\left[1 - \frac{B(\ell)}{B_m}\right]^{1/2}$ where $\ell = 0$ at the equator. The maximum distance from the equator corresponds to the value ℓ_m where $B(\ell_m) = B_m$. The time interval needed to go from one mirror point (M_1) to the other (M_2) is given by

$$(4.23) \quad T_b = 2\int_{M_1}^{M_2} \frac{d\ell}{v_{\parallel}(\ell)} = \frac{2}{v}\int_{\ell_1}^{\ell_2} \frac{d\ell}{\left[1 - \frac{B(\ell)}{B_m}\right]^{1/2}}$$

It is easy to show that particles having pitch angles close to 90° on the equator experience a harmonic bounce motion with a period $T_b \approx \frac{2\sqrt{2}\,\pi}{v}\left(\frac{B_0}{a_0}\right)^{1/2}\left(1+\mu_0^2/2\right)$ where μ_0 is the value of $\cos\alpha_0$ (achieved at the equator) and $a_0 = \left(\frac{d^2B}{d\ell^2}\right)_{equator}$

4.2.2.1. First of all we shall derive the average of the motion equation parallel to the magnetic field taken over a cyclotron rotation period, to look for the motion of the guiding center. The (slowly) variable field $\underline{B}$ over the circular orbit can be written as $\underline{B} = \underline{B}_c + \underline{b}$ where $\underline{B}_c$ is the field at the guiding center and $\underline{b}$ the small perturbation to add in the actual position of the drifting particle. The motion equation is thus:

$$(4.24) \quad m a_{\parallel} = e(\underline{v} \times \underline{b})_{\parallel} + eE_{\parallel} + F_{\parallel}$$

where

$$(4.25) \quad \begin{cases} a_{\parallel} = \frac{dv_{\parallel}}{dt} - \underline{v}\cdot\frac{d\underline{u}}{dt} & \underline{u} = \underline{B}/B \\ \underline{v} = \underline{v}_{\parallel} + \underline{V}_D \end{cases}$$

($v_{\parallel}$ is $\approx$ constant over a cyclotron period)

so that the average of $a_{\parallel}$ is given by

$$(4.26) \quad \langle a_{\parallel}\rangle = \frac{dv_{\parallel}}{dt} - v_{\parallel}\,\underline{v}\cdot\frac{d\underline{u}}{d\ell} = \frac{dv_{\parallel}}{dt} - v_{\parallel}\,\underline{V}_D\cdot\frac{\nabla_{\perp}B}{B}$$

The first term on the right side of (4.24) can be written as

$$e(\underline{v}\times\underline{b})_{\parallel} = e(\underline{v}_{\parallel} + \underline{v}_{\perp})\times(\underline{b}_{\parallel} + \underline{b}_{\perp}) = e(\underline{v}_{\perp}\times\underline{b}) = e\,\underline{v}_{\perp}\times\underline{b}_r$$

Where $\underline{b}_r$ is the field component oriented along the radius of the orbit. For small r one can use $b_r = kr$ with $k = \frac{1}{2}\nabla_{\parallel}B$

so that the average of (4.24) over the cyclotron period becomes

$$(4.27) \quad m\frac{dv_{\parallel}}{dt} = eE_{\parallel} + F_{\parallel} - e v_{\perp}\frac{1}{2}\nabla_{\parallel}B\,\rho_c + m v_{\parallel}\underline{V}_D\cdot\frac{\nabla_{\perp}B}{B}$$

which is valid under the condition $\varrho_c \frac{\nabla_{\parallel} B}{B} \ll 1$ where ϱ_c is the gyroradius.

If the last term can be neglected (as it is usual) and because of the constance of magnetic moment μ ~~equation~~ (4.27) finally becomes

$m \frac{dv_{\parallel}}{dt} = -\frac{\partial}{\partial l}\left[U(l) + \mu B(l)\right]$ where U is the potential of all forces.

~~We now derive the energy equation to describe~~ As regards the rate of change of the kinetic energy T in a time dependent field, not going into details, we only indicate its rate of change:

$$(4.28) \quad \frac{dT}{dt} = \mu \frac{\partial B}{\partial t} + \left(\underline{v}_{\parallel} + \underline{V}_0\right)\cdot\left(e\underline{E} + \underline{F}\right)$$

which can be simply interpreted. The first term on the right hand describes the betatron acceleration, and the second term the work by the forces acting on the drifting particle. A special case of (4.28) occurs when the temporal variability of $\underline{B}$ is due to the motion of the static field embedded in a plasma cloud: in this case the acceleration process is called Fermi acceleration.

4.2.2.2. During the bounce motion each particle experiences a drift. If the drift is very slow, of the order of one gyroradius during a bounce period, we can give a simple geometrical description of the motion introducing the concept of drift shell made by all field lines along which progressively a particle bounces because of the simultaneous drift motion. An average drift velocity $\langle v_o \rangle$ of the field line over which the particle bounces can be obtained with reference to a given surface everywhere perpendicular to the local

field line (for the dipole case one such surface coincides with its equatorial plane). Actually

$$\langle \underline{v}_o \rangle = \frac{2}{T_b} \int_{l_1}^{l_2} \underline{v}_{ol} \frac{dl}{v_{\parallel}}$$

where again l_1, l_2 are the curvilinear coordinates at the opposite mirror points and $\underline{v}_{ol}$ is the drift velocity of the intersection point of the field line along which the particle at distance l is istantaneously in motion on the reference surface. The drift velocity $\underline{v}_l$ at distance l, given by the sum of the force drift $\underline{V}_F$ and the combined gradient and curvature drifts, can be transformed into the corresponding velocity $\underline{v}_{ol}$ on the reference surface by means of simply geometrical relationships once the field line structure is given. The bounce average velocity becomes

$$(4.30) \quad \langle \underline{v}_o \rangle = \frac{1}{T_b}\left(\frac{\underline{\nabla} J \times \underline{B}}{-eB^2}\right)_o$$

where $J = \oint p_{\parallel}\, dl = \oint p \cos\alpha\, dl$ and the subscript indicates that all quantities are computed at the intersection points.

The integral J can also be written as J = 2pI (in absence of parallel forces and for small temporal variations over a bounce period) with $I = \int_{l_1}^{l_2}\left[1 - \frac{B(l)}{B_m}\right]^{1/2} dl$, only dependent upon the field geometry. Equation (4.30) states that $\langle v_o \rangle$ is normal to the vector $\underline{\nabla} J$, i.e. parallel to the surface J = const. This implies that J is an adiabatic invariant: when the field is static, I is constant, in addition to B_m=const. When external forces perpendicular to the magnetic field are present (i.e. the lines are equipotential) it can be shown that the product $K = I\, B_m^{1/2}$ is constant. This is no longer true when the external forces have parallel components.

4.3. The third adiabatic invariant.

The drift motion of particles on closed shells can be described in some situations not requiring exactly where the individual particles are located at a certain time, but rather only knowing the drift shell on which they are in motion. With a static field the drift is periodic with a period $T_d = \oint \frac{dl}{\langle v_o \rangle}$ where the line integral is computed along the closed drift orbit laying on the drift shell. In the presence of a temporal field variations an induced electric field is generated and particles are driven to new shells. At any given time a particle can be considered drifting on a certain transient shell, which acts as instantaneous guiding drift shell. In the case of a static field the guiding drift shell is the actual drift shell over which the particle is driven. Motion from one shell to another implies a change of particle energy, described by equation (4.28). In the extreme case of a time variation of the field very slow compared to the drift period $\left(T_{drift} \ll \frac{B}{\frac{\partial B}{\partial t}}\right)$ a third parameter happens to be adiabatically invariant. It is quite obvious that fulfillment of the above condition is dependent

upon the particle energy. At lower energy the drift period increases, so to make more difficult the validity of the condition. Actually, under slow temporal variations, it can be shown that the magnetic flux encompassed by the guiding drift shell of a particle is constant. This statement is mathematically expressed by the equation

$$\Phi = \oint \underline{A}_o \cdot \underline{dl} = \text{const} \tag{4.31}$$

where $\underline{A}_o$ is the magnetic vector potential. The integral is computed on a closed line lying on the guiding drift shell under constant field intensity. The particle motion occurs on a closed shell whose shape is slowly changing with time.

4.4. The motion of a charged particle in a dipole field (Störmer's theory).

This problem was extensively studied by Störmer in the first decade of our century in view of a theory of the polar aurora. It was recognized later that the Störmer theory had much more to do with cosmic rays and with the more recently discovered radiation belts than with aurora. We shall give an outline of the basic concepts. In the basic equation of motion (4.1) the cylindrically symmetrically dipole field plays a simplifying role. Using cylindrical coordinates (ρ, φ, z) and taking a dipole $\underline{M} \parallel \underline{z}$ the field $\underline{B}$ can be written as:

$$\underline{B} = (\underline{\phi} \times \underline{\nabla} U)/\rho \tag{4.32}$$

where $\underline{\phi}$ is the unit vector in the direction of increasing azimuth φ, $\mathcal{V} = M\rho^2/r^3$ and the field lines equation is $\mathcal{V}$=const, φ=const.
Constanty of the velocity v implies that d/dt = vd/ds s being the curvilinear coordinate along the trajectory, so that the motion equation becomes

$$(4.33)\quad \frac{d^2\underline{r}}{ds^2} = \frac{e}{mv}\left(\frac{d\underline{r}}{ds}\times\underline{B}\right)$$

It is straighforward to transform this equation into

$$(4.34)\quad \frac{1}{C_{st}^2}\frac{d^2\underline{r}}{ds^2} = \frac{d\underline{r}}{ds}\times\left[\underline{\phi}\times\frac{1}{\rho}\nabla\left(\frac{\rho^2}{r^3}\right)\right]$$

where $C_{st} = \left(\frac{eM}{mv}\right)^{1/2}$ is a constant length (Stormer's constant).
A useful dimensionless expression of above equation is obtained expressing all lengths in terms of C_{st}:

$$(4.35)\quad \frac{d^2\underline{r}}{ds^2} = \frac{d\underline{r}}{ds}\times\left[\underline{\phi}\times\frac{1}{\rho}\nabla\left(\frac{\rho^2}{r^3}\right)\right]$$

which implies that the same family of orbits describes the motion of different particles of the same sign and different strengths of the dipole.

Using a simple vector identity(*) the above equation can be written as

$$(4.36)\quad \frac{d^2\underline{r}}{ds^2} = -\frac{1}{\rho}(\underline{t}\cdot\underline{\phi})\nabla\frac{\rho^2}{r^3} + \frac{1}{\rho}\frac{\partial}{\partial s}\left(\frac{\rho^2}{r^3}\right)\underline{\phi}$$

(*) $\underline{A}\times(\underline{B}\times\underline{C}) \equiv \underline{B}(\underline{A}\cdot\underline{C}) - \underline{C}(\underline{A}\cdot\underline{B})$

where $\underline{t}$ = d$\underline{r}$/ds is the unit vector tangent to the trajectory. The φ-component of this equation can be simply written, taking advantage of the null φ component of the field potential,

$$(4.37)\quad \frac{1}{\rho}\frac{d}{ds}\left(\rho^2\frac{d\phi}{ds}\right) = \frac{1}{\rho}\frac{\partial}{\partial s}\left(\frac{\rho^2}{r^3}\right)$$

from which an integral of the motion is immediately obtained

$$(4.38)\quad \rho^2\frac{d\phi}{ds} = \frac{\rho^2}{r^3} + 2\gamma$$

where γ is an arbitrary integration constant. The above expression describes the azimuthal motion of the particle. Important consequences can be derived from equation (4.38) which can be furtherly written as

$$(4.39)\quad \operatorname{sen}\vartheta = \rho\frac{d\phi}{ds} = \frac{2\gamma}{\rho} + \frac{\rho}{r^3}$$

The limitation introduced by the sin ϑ implies that there are regions of space from which the trajectories are excluded. As discussed extensively by Störmer, three different cases can be distinguished according to the value of γ. Positive values imply that no trajectory exists through the origin; when $-1<\gamma<0$ there are trajectories connecting infinity to the origin; finally in the case $\gamma<-1$ tranjectories through the origin and trajectories at infinity are no longer connected: in other words, no particle approaching the dipole from infinity is allowed within a certain "forbidden" region centered at the dipole itself and, on the other hand, a closed region exists around the dipole such that no particle inside it can go to infinity. Using today's nomenclature this is a region which any particle contained in it can never leave (unless external forces perturb ~~their~~ its orbit): particles are "trapped" (fig. 10 and 11). In any case, the actual shape of a particle orbit is very complicate and, except a very few special cases, only numerical integration of the motion equation can be performed to know the orbit.

4.5. The Liouville's Theorem.

This is an important theorem which allows to know some properties of a particle distribution in one place in terms of those elsewhere. In the six dimension space (phase space) where the coordinates of a particle are the three geometrical coordinate x_i $(i=1,2,3)$ and the corresponding three momenta p_i $(i=1,2,3)$ the particle density N variations are obviously expressed by

$$(4.40)\qquad -\frac{\partial N}{\partial t} = \mathrm{div}(N\underline{v}) = \sum_{i=1}^{6}\frac{\partial N}{\partial x_i}\dot{x}_i + N\sum_{i=1}^{6}\frac{\partial \dot{x}_i}{\partial x_i}$$

or,

$$\frac{dN}{dt} = -N\sum_{i=1}^{6}\frac{\partial \dot{x}_i}{\partial x_i}$$

By introducing the Hamiltonian H and the known relationships

$\dot{x}_i = \frac{\partial H}{\partial p_i}$ $\quad \dot{p}_i = -\frac{\partial H}{\partial x_i}$ one immediately gets

$$(4.41)\qquad \frac{dN}{dt} = 0$$

which means that in the phase-space the particle density N is conserved along a dynamic trajectory, i.e. it has ~~that~~ the same value at each point of the trajectory.

The Liouville's theorem which also holds in the case of charged particles in a electromagnetic field is extremely important in the description of the entrance of cosmic rays into the geomagnetic field and of trapped particles. In particular, if J is the differential unidirectional particle flux, i.e. the number of particles per unit time, unit energy, unit area, unit solid angle we can write (because of the relationship $J\,dt\,dE\,dS\,d\Omega = Nv\,dt\,dS\,p^2dp\,d\Omega$)

$$(4.42)\qquad J = Nvp^2$$

In the case only a static magnetic field exists, v and p are constant so that Liouville's theorem implies that J = constant. It is necessary to stress the point that correct use of the theorem requires data from a detector with infinitesimal cross section and solid angle: in other words, the theorem is not straightforwardly applicable to measurements by omnidirectional detectors.

4.6. Special magnetic coordinates.

Following the discovery of the radiation belts it was early recognized the need of an appropriate reference system to organize the observations. The unidirectional flux J, in general, is a function of r, v, t. However, constancy of the three adiabatic invariants (when applicable) and use of Liouville's theorem allows important simplifications. First of all, at the mirror points we have an unidirectional flux $J_\perp = J_\perp(r,v)$ where v is the constant velocity of the particles on their circular trajectory. On the other hand, once the point r is defined, also the values of the three adiabatic invariants are defined. Constancy of the unidirectional flux $J_\perp$ during the azimuthal drift implies it is also the same at any longitude so we can state that $J_\perp$ only depends upon the adiabatic invariants μ, I, Φ.

For the simple case of a dipole $\underline{M}$ the expressions for μ, I and Φ are given by

$$\text{(4.43)} \quad \begin{cases} \mu = E/B_m \\ I = L_D\sqrt{E}\, f(B_m, L_D) = J/2p \\ \Phi = \dfrac{2\pi M}{L_D} \end{cases}$$

where L_D is the equatorial distance of a line of force of the dipole and $f(B_m, L_D)$ is an integral computed along the field line between the mirror points. Now, using the spherical harmonics expression of the actual non-dipolar field it is still possible to define a length L satisfying the equation

$$\text{(4.44)} \quad I = L\sqrt{E}\, f(B_m, L)$$

where the function f is the same applicable to the case of the purely dipolar field. In conclusion a new parameter L is defined, depending upon B_m and $I/\sqrt{E}$, which would be exactly constant in the dipole case while in the real case happens to be nearly constant, within 1% along the real lines of force. This also means that $J_\perp$ can also be written as $J_\perp(E, B_m, L)$. The so-called McIlwain coordinate system is accordingly defined, by analogy with the dipolar case by means of two new coordinates, the distance r' and the latitude λ'

expressed by the equation (valid for the dipole)

$$\text{(4.45)} \quad \begin{cases} B_m = \dfrac{M}{r'^3}\left[4 - 3\dfrac{r'}{L}\right]^{1/2} \\ \cos^2\lambda' = r'/L \end{cases}$$

M being the dipole moment.

4.7. The response of omnidirectional particle detectors.

Most of the measurements are made by means of directional instruments; since the lines of force play an essential role in the motion of the trapped particles, we shall express the particle fluxes along a field line.

In general, the particle flux in a given point depends upon the field B, the parameter L and the so-called pitch angle α which is the angle of the velocity vector to the vector $\underline{B}$. Because Liouville's theorem we can say that

$$J(L, B, \alpha) = J_\perp(L, B_0)$$

or, introducing a parameter $\xi = B/B_0 = BL^3/M$

$$\text{(4.46)} \quad J(L, \xi, \alpha) = J_\perp(L, \xi_m) \text{ with } \xi_m = BM/B_0$$, i.e. the value of ξ at the mirror points. In a similar way, the same flux can also be expressed by means of the unidirectional equatorial flux at an angle α_0 such that $\sin^2\alpha_0 = B_m \sin^2\alpha / B$.

Complete information on a given trapped particle distribution around a given field line can be obtained by a set of perpendicular flux measurements along the line or, and better, by measuring unidirectional fluxes at the equator, which is possible at only one place and in a very short time interval. If one looks at omnidirectional fluxes, the Liouville's theorem is not immediately applicable, so that ~~does not hold~~ (more complicate expressions are needed. By definition the omnidirectional flux $\mathbf{J}(L,\xi)$ is given by

$$(4.47)\quad \mathbf{J}(L,\xi) = \int_0^{4\pi} J(L,\xi,\alpha)\, d\Omega = 4\pi \int_0^1 J(\cdot\cdot)\, d\cos\alpha$$

where the obvious hypotheses that J does not depend upon the azimuthal and $J(\alpha)=J(\pi-\alpha)$ have been used.

The differential of $\cos\alpha$ can be easily expressed by means of the differential of $\cos\alpha_0$ at the equator. So that

$$(4.48)\quad \mathbf{J}(L,\xi) = 4\pi\xi \int_{\sqrt{1-1/\xi}}^{1} J(L,\alpha_0)\, \frac{\cos\alpha_0\, d\cos\alpha_0}{[1-\xi\, \mathrm{sen}^2\alpha_0]^{1/2}}$$

Proceeding in the opposite way, it is similarly possible to express $J(L,\alpha_0)$ by means of $\mathbf{J}(L,\xi)$ as follows

$$(4.49)\quad J_\perp(L,\xi_m) = -\frac{\xi_m^{3/2}}{\pi} \int_{\xi_m}^{\xi^*} \frac{\frac{d}{d\xi}\left(\frac{\mathbf{J}(L,\xi)}{2\pi\xi}\right)}{\xi-\xi_m}$$

where ξ^* is the limiting value of ξ such that $J(L,\xi)=0$ for $\xi<\xi^*$ (the value ξ^* is to be located somewhere in the upper atmosphere where total particle absorption occurs). The obvious condition $\xi>\xi_m$

(4.49) indicates that the expression is computed by knowing the values of $J(L,\xi)$ at points closer to the origin than the point ξ_m.

One last comment is worth about the pitch angle distributions. All particles having their mirror point at L,ξ^* have at the equator a pitch angle α_0^* such that $\mathrm{sen}^2\alpha_0^* = 1/\xi^*$. This also means that all particles having an equatorial pitch angle $\alpha_0<\alpha_0^*$ are lost in their penetration at altitudes below that corresponding to the point ξ^*. The cone, centered on the field line, with an angular width α_0^* is called "loss-cone" to emphasize that particles contained in it at the equator are going to be lost from the distribution. The actual integral flux in the loss cone must be computed taking into account the effect due to the convergence of the field lines approaching Earth. So, it is expressed by

$$(4.50)\quad N = \int_0^{4\pi} J(L,\xi,\alpha)\, d\Omega$$

In the simple case of an isotropic flux $J_0(L)$ at the equator, we then have $N = 4\pi J_0(L)$ (and not $N=J_0(L)\cdot\Omega^*$, with Ω^* ~~is~~ the solid angle of the loss cone, which is less than the real flux obtained by correct use of Liouville's theorem).

5. The interaction of solar wind with the geomagnetic field.

5.1 The permanent ~~corpuscular~~ particle flux from the Sun, called solar wind by Parker, determines profound modifications of the near Earth magnetic and particle environment. The very first correct approach to the problem is that by Chapman and Ferraro, who in the early thirties put the foundations of what is now called plasma physics. Their starting idea was that a stream of charged particles, positive and negative with zero total charge density, was reaching the Earth in coincidence with geomagnetic storms. We now know that ~~the existence of~~ a permanent solar particles flux is flowing from the Sun through the interplanetary space, with variable velocity and particle density, typically several hundreds km/sec and a few ~~tens~~ particles/cm^3. The flux is typically of the order of a few 10^8 particles/cm^2/sec. In general, the solar wind approaches the Earth with a velocity either supersonic or superalfvenic (fig. 12). So the conditions exist for the generation of a shock at some distance from Earth.

It is instructive to look first at a qualitative description of the physical situation close to Earth. To this end a classical problem solved by Maxwell more than one century ago may help: it is the problem of a conductive rigid plane approaching a dipole magnetic field and parallel to the dipole moment. Under these circumstances, which are reasonably representative of what happens in the very initial phase of a geomagnetic storm, a current system is generated by electromagnetic induction. The magnetic field associated with the current system modifies the field topology in such a way that in the limit of a conductivity of the surface going to infinity the magnetic field lines are compressed in front of the advancing plane and pushed away to the back. The model ~~does not work as well~~ may help somewhat to understand qualitatively what happens (when the conducting plane is not ~~taken as~~ rigid, which ~~is~~ actually resembles the case of a charged particle stream impinging on Earth. Other complications are due to the fact that (i) the flux of particles emitted from the Sun is actually a permanent feature with an embedded magnetic field of solar origin (the so-called frozen-in field) whose lines may or may not be connected with the geomagnetic field lines (see section 6); (ii) dissipation processes are present and, (iii) anysotropic and multi-component plasma is to be assumed. In these conditions, one can give a qualitative description saying that a separation surface is to be expected beyond which, on the interplanetary side, an umperturbed solar wind flux is observed, an internal surface inside which the geomagnetic field lines are confined (although modified in shape and direction); the two surfaces are separated by a region where a number of complex physical phenomena takes place. The external surface must have the characteristics of a shock, the inner surface (called magnetopause) is a discontinuity surface which under simplyfying conditions is parallel to the distorted geomagnetic field lines. The intermediated region, called magnetosheath is a transition region inside which the impinging solar wind, unable to penetrate the inner region of the magnetosphere, flows around the obstacle ~~[illegible]~~ and magnetohydrodynamic turbolence plays an important role.

It is necessary at this point to formulate the problem in a more quantitative way, writing the basic equations.

Assuming the steady case and a non dissipative perfect (compressible) gas (electrically perfectly conducting, non viscid, non heat-conducting) one can write the following equations

$$\text{(5.1)} \quad \underline{\nabla} \cdot \rho \underline{v} = 0 \qquad \text{(continuity equation)}$$

$$\text{(5.2)} \quad \rho (\underline{v} \cdot \underline{\nabla}) \underline{v} = -\underline{\nabla} p + \frac{1}{4\pi} \underline{J} \times \underline{H} = -\underline{\nabla} p - \underline{H} \times \text{curl}\, \underline{H} / 4\pi =$$

$$= -\underline{\nabla} p - \frac{1}{8\pi} \underline{\nabla} H^2 + \frac{1}{4\pi} (\underline{H} \cdot \underline{\nabla}) \underline{H} \qquad \text{(motion equation)}$$

where the acting forces are pressure gradient and magnetic forces on the current density J

$$(5.3)\quad \nabla\cdot \underline{H} = 0$$ (solenoidal field condition)

$$(5.4)\quad \mathrm{curl}\,(\underline{H}\times \underline{v}) = 0$$ (frozen-in field condition)

$$(5.5)\quad (\underline{v}\cdot\underline{\nabla})\, S = 0$$ (entropy equation) equivalent to

the energy equation

$$(5.6)\quad \underline{\nabla}\cdot\left[\rho \underline{v}\left(\frac{1}{2}v^2 + h\right) + \frac{\underline{v}}{4\pi}H^2 - \frac{1}{4\pi}(\underline{H}\cdot\underline{v})\,\underline{H}\right] = 0$$

In the above equations ρ, p, S, $\underline{v}$, h are density, pressure, entropy, velocity and enthalpy of the gas, $\underline{H}$ is the magnetic field; The familiar pressure density relationship ~~[illegible]~~ is also to be added.

~~[illegible]~~

Neglect of dissipative terms, which contain second derivatives, requires the assumption of small first derivatives (or gradients). As a consequence, any time a gradient tends to increase beyond certain limits (which happens to be the case close to the shock and the magnetopause), the above equations break down, although they remain valid on the two sides of the critical, thin, region where gradients are big. In other words ~~or~~ physical discontinuities occur.

It is immediate, thus, to write down the conservation relations between quantities on the two sides corresponding to above equations. A useful set of relations can be written by introducing some appropriate symbols, in particular mean values $\langle a\rangle = (a_0+a_1)/2$, variations $[a]=[a_1-a_0]$, the specific volume $V = 1/\rho$ and $m = \rho v_n$. (The mass flux normal to the discontinuity surface)

The relationships at the discontinuity can thus be written as follows:

$$(5.7)\quad m\,[V] - [v_n] = 0$$

$$(5.8)\quad m\,[\underline{v}] + [p]\,\underline{n} + \frac{1}{4\pi}\langle \underline{H}\rangle\cdot[\underline{H}]\,\underline{n} - \frac{1}{4\pi}H_n\,[\underline{H}] = 0$$

$$(5.9)\quad m\,\langle V\rangle\,[\underline{H}] + \langle \underline{H}\rangle\,[v_n] - H_n\,[\underline{v}] = 0$$

$$(5.10)\quad [H_n] = 0$$

$$(5.11)\quad m\left\{\left[e + \frac{VH^2}{8\pi}\right] + [V]\left(\langle p\rangle + \frac{1}{8\pi}\langle \underline{H}_t^2\rangle - \frac{1}{8\pi}H_n^2\right) - \frac{1}{4\pi}[V\underline{H}_t]\cdot\langle \underline{H}_t\rangle\right\} = 0$$

where $\underline{n}$ is the unit vector normal to the discontinuity plane.

As a whole, the above vector equations correspond to nine scalar equations in nine variables $[V]$, $[p]$, $[\underline{v}]$, $[\underline{H}]$, $[e]$ one of which trivially defined by $[H_n] = 0$.

The set of homogeneous equations (5.7 to 5.11) is compatible if the determinant of coefficients is zero, i.e. if

$$(5.12)\quad \langle V\rangle^2 m\left(\langle V\rangle m^2 - \frac{H_n^2}{4\pi}\right)\left\{\langle V\rangle m^4 + \left(\frac{\langle V\rangle}{[V]}[p] - \frac{\langle H\rangle^2}{4\pi}\right)m^2 - \frac{[p]}{[V]}\frac{H_n^2}{4\pi}\right\} = 0$$

Solutions of above equations can be obtained straightforwardly. The solution $m_1=0$ corresponds to the so-called "tangential" and "contact" discontinuities, characterized by zero flux of particles through the discontinuity plane.

The solutions $m_{2,3} = \pm H_n/(4\pi\langle V\rangle)^{1/2}$ correspond to the so-called "rotational" discontinuities, while the other four solutions are usually associated to the so-called "shock-waves". These solutions, coming from the third factor of (5.12), put $=0$ ~~equation~~ can be discussed rewriting the equation in a somewhat different way

$$(5.13)\quad \left(m^2 + [p]/[V]\right)\left(\langle V\rangle m^2 - H_n^2/4\pi\right) = m^2\langle H_t^2\rangle/4\pi$$

from which it follows that the two possibilities $m^2 > m_r^2$ or $m^2 < m_r^2$ with $m_r^2 = H_n^2/(4\pi\langle V\rangle)$ imply respectively

$$m^2 > -[p]/[V] \quad \text{and} \quad m^2 < [p]/[V]$$

The solutions corresponding to the case > are called <u>fast shock</u> waves; those corresponding to the case < are <u>slow shock</u> waves. The relationships between physical quantities on the two sides of the shock wave can finally be put in the form

$$[\underline{H}_t] = [\underline{H}] = -\frac{m^2 [V] \langle \underline{H}_t \rangle}{\langle V \rangle m^2 - H_n^2/4\pi}, \quad [H_n] = 0, \quad [\underline{H}]^2 = 2\langle \underline{H} \rangle \cdot [\underline{H}]$$

$$[\underline{v}_t] = -\frac{m [V] H_n \langle \underline{H}_t \rangle / 4\pi}{\langle V \rangle m^2 - H_n^2/4\pi}, \quad [v_n] = -[V] m, \quad [V] < 0, \quad [\rho] > 0 \tag{5.14}$$

It follows immediately that $\underline{H}_t$ and H^2 increase (decrease) through a fast (slow) shock.

A discussion of all implications of above equations is to be found in the original papers. Here we only like to make an important point, i.e. that if the inertial term $\rho(\underline{v}\cdot\underline{\nabla})\underline{v}$ is much larger than the magnetic term $\frac{1}{4\pi}\underline{H} \times \mathrm{curl}\,\underline{H}$ in the motion equation, this last can be dropped and the result is that a decoupling of dynamical and magnetic terms occurs so that the solution of the basic equations can be obtained solving first the simpler gasdynamic case and then using the equations containing the magnetic field in which the velocity of the fluid motion is no longer an unknown, since it is given by the dynamic solution. In other words, we can think in terms of magnetic field lines convected by the fluid (similarly to a line of smoke slowly diffusing into and convected by a fast moving fluid). Introduction of some approximations may lead to further simplifications when computing the shape of the magnetospheric boundary (what we already called magnetopause). The boundary behaves as a tangential discontinuity for which among others conditions the total magnetic + dynamic pressure $p + \frac{H^2}{8\pi}$ must be continuous; if one notices that on the external side the dynamic pressure overhelms the magnetic pressure, it becomes possible to approximate the external pressure by means of

$$p \approx k \rho_\infty v_\infty^2 \cos^2 \psi$$

where ψ is the angle of the asymptotic flux velocity v_∞ with the magnetospheric boundary, ρ_∞ is the asymptotic charged particle density and k is a factor of the order of unity (actually k = 2 for specular reflection; k = 1 if particles are absorbed). The second step has been that of substituting the condition $H_n = 0$ at the magnetospheric boundary by the statement that the tangential field, is given by $H_t = 2f(H_{dipole})_t$, where f is of the order of 1 and $(H_{dipole})_t$ is the dipole field component tangent to the surface. This condition was originally found as valid at the boundary of the conducting plane approaching Earth, considered by Chapman and Ferraro, as earlier pointed out.

Introducing the familiar expression of the geomagnetic field and neglecting the dynamic pressure inside the boundary it is possible to write a partial differential equation connecting the distance r from the Earth's center to the latitude and longitude at each point of boundary. A general expression of this equation valid for <u>all</u> the boundary (not only for certain special meridian intersections!) is due to Spreiter and Jones (1962).

Once the shape of the magnetosphere (or geomagnetic cavity) has been computed, the next step is that of determining the dynamic flow around the obstacle (assumed as symmetric around the Sun-Earth direction: although this is not exactly true still it is a reasonable working approximation.

Several techniques have been used by different authors to solve the problem, which, however, at this stage goes much beyond the scope of this review. Here we limit ourselves to show some results in graphical form (fig. 13, 14, 15) to allow a feeling of what the real situation is. Another important feature coming out of the models is that a bundle of magnetic field lines, those leaving the north magnetic pole or entering the south pole are completely displaced a few Earth's radii above its surface and pushed back into the antisolar direction to build what from the very beginning was called "geomagnetic tail". In principle, the fast decrease of the geomagnetic field and hence of the magnetic pressure in the presence of the solar wind dynamic pressure would imply a short geomagnetic tail which would close as rapidly as the thermal pressure of the solar wind becomes prevailing. Actually this ~~is~~ does not (seem to be) the case, since the tail is well observable as far as 1000 Earth's radii, which means that in one way or another a particle pressure is present to balance the inward tension of the magnetic field.

In the following section, rather than going into the complications outlined above we shall consider an elementary view of the large-scale interactions which although in ~~some~~ several respects are oversimplified, ~~however~~ nevertheless have the advantage of being analytically workable and thus capable to illustrate the basic ideas of the coupling of the magnetosphere with the surrounding medium.

6. ~~SOME~~ SIMPLE MODELS IN MAGNETOSPHERIC PHYSICS

6.1. The case of symmetric models.

The basic features of the magnetosphere can be illustrated in a qualitative (and also quantitative, in some cases) way by means of simple models which have the advantage of being mathematically expressed by workable analytical expressions.

This is expecially appropriate to clarify some basic ideas, which will ~~studied~~ be presented and discussed in more detail in the second ~~part~~ series of ~~this course~~ lectures on magnetosphere by prof. Roederer.

Two basic equations to keep in mind for a perfectly conducting gas as the solar wind are the so-called magnetohydrodynamic condition and the frozen-in field equation, namely

$$\underline{E} = -\underline{v} \times \underline{B} \tag{6.1}$$

and

$$\frac{\partial \underline{B}}{\partial t} = \underline{\nabla} \times (\underline{v} \times \underline{B}) \tag{6.2}$$

The second of these equations can be straightforwardly be used to show its equivalence to the condition of the conservation of the magnetic flux threading a closed line such that each point of it moves at the bulk velocity; this also implies that any particles sharing a same line of force will continue to do the same at any other time, or in other words, the lines of force are convected by the plasma in motion, frozen in it.

Let us consider now the physical consequences of the interaction of a magnetic field $\underline{B}_{SW}$ convected by the solar wind and the geomagnetic field (considered as a dipole field, which is a good approximation for our proposes).

We shall assume $\underline{B}_{SW} = B_0 \underline{z}$

where $\underline{z}$ is the unit vector parallel to the dipole moment $\underline{M}$ and B_0 is the field component along the z axis, ~~which points~~ northward if B_0 is >0 and southward if B_0<0. If the boundary conditions are that $\underline{B}$ tends to B_{SW} or to B_{dipole} respectively when the distance r from the center of dipole tends to infinity or to 0, we can write the resultant magnetic potential V as

$$(6.3) \qquad V = V_{SW} + V_{dipole} = -B_0 z - \frac{M\cos\vartheta}{r^2}$$

where ϑ is the colatitude referred to the dipole orientation. Now the field can also be written, by means of the so-called eulerian potentials α, β, as $B = \nabla\alpha \times \nabla\beta$ where the contribution from the dipole is described by

$$(6.4) \qquad \begin{cases} \beta = a\varphi \\ \alpha = -aB_e\left(\frac{a}{r}\right)\operatorname{sen}^2\vartheta \end{cases}$$

Where a is the Earth's radius and B_e the equatorial field; the contribution from the solar wind field is described by

$$(6.5) \qquad \begin{cases} \beta = a\varphi \\ \alpha = \frac{aB_0}{2}\left(\frac{r}{a}\right)^2\operatorname{sen}^2\vartheta \end{cases}$$

In this special case, due to common expression for β, we can write the resultant potentials by means of

$$(6.6) \qquad \begin{cases} \beta = a\varphi \\ \alpha = a\operatorname{sen}^2\vartheta\left[\frac{B_0}{2}\left(\frac{r}{a}\right)^2 - B_e\left(\frac{a}{r}\right)\right] \end{cases}$$

Let us now discuss the implications of this expression.

First of all $\alpha = 0$ implies $\left(\frac{r}{a}\right)^3 = 2B_e/B_0$ so that a physically possible value only exists if $B_0>0$ in which case $\alpha=0$ on a sphere of radius $r = a\left(\frac{2B_e}{B_0}\right)^{1/3}$, which with $B_e=30.000\ \gamma$ $B_0 = 5\gamma$ means $r \cong 23$ a. On this sphere the radial field component $B_r=0$, i.e. the vector B is everywhere parallel to it: two (fig.16)

kinds of field lines thus exist, closed lines inside the sphere i.e. purely terrestrial lines, and open distorted field lines outside, i.e. purely interplanetary lines. The sphere encloses a region which has several characteristics of a closed magnetosphere inside which the field lines are confined, although modified in shape. The field strength B is zero in two opposite points (called neutral points on the intersection of the sphere and the dipole axis. An equivalent view point is that a current system is produced on the sphere through which the field is discontinuous. Different configurations, as regards the orientation of the open field lines can occur if the field B_{SW} is oriented in other directions.

The field topology (fig.17) is substantially different in the case $B_0<0$. First of all the sphere found above no longer exists; the radial field component is everywhere zero but the z component only vanishes on a circular line defined on the equatorial plane by

$$(6.7) \qquad -B_0\left(\frac{r}{a}\right) + B_e\left(\frac{a}{r}\right)^2 = 0$$

which is satisfied by $r = a\left(\frac{B_e}{B_0}\right)^{1/3}$.

~~namely at r = a~~

It is interesting to remark that also an electric field distribution is associated with the above changes of the magnetic field configuration. The incoming solar wind with a bulk velocity $\underline{v}$ must be permeated by an electric field $\underline{E} = -\underline{v}\times\underline{B}_\circ$ if it has to advance toward the Earth with the velocity $\underline{v}$. The fact that $\underline{E}$ is normal to $\underline{B}_\circ$ means that no restriction is put on the longitudinal component $E_{\parallel}$ which usually is taken as vanishing, due to the high electric conductivity along the field lines which immediately nullifies any potential difference along the field lines.

Let us put $\underline{v} = -v_\circ \underline{x}$ where $\underline{x}$ is the unit vector from Earth to Sun; viewed from an Earth centered reference system, where particles drift at a velocity

$$(6.8) \qquad v_{drift} = \underline{E}\times\underline{B}/B^2$$

It is quite obvious that the drift velocity will be significantly perturbed in proximity of the Earth. It is then interesting to understand what happens. Let us look in particular to the electric field $\underline{E}$. As remarked above the simplifying assumption ~~based on the high conductivity of the field lines is~~ that the electric potential on the field lines is constant (case $B_\circ>0$) can be made, so that the potential distribution close to the sphere $r=r_\circ$ is simply determined by projecting along the field lines the potential Φ existing at other place, in particular at infinity. The vectors $\underline{B}$ and $\nabla\phi$ are perpendicular to each other $(\underline{B}\cdot\underline{\nabla}\phi=0)$. The function $\Phi(x,y,z)$ can also be expressed by means of two functions of (x,y,z), i.e. for example by the two eulerian potential α and β.

Now as r goes to infinity we can write the potential

$$(6.9) \qquad \alpha = \frac{aB_\circ}{2}\,\mathrm{sen}^2\vartheta\left(\frac{r}{a}\right)^2$$

We also have $\underline{E} = -\underline{\nabla}\Phi$ where $\Phi = y\, v_\circ B_\circ$

so that $\alpha_\infty = \frac{B_\circ}{2a}\, y^2/\mathrm{sen}^2(\beta/a)$

This means that

$$(6.10) \qquad \Phi(\alpha,\beta) = v_\circ (2a_\circ B_\circ)^{1/2}\alpha^{1/2}\,\mathrm{sen}(\beta/a)$$

If we now take the complete expression of α it is possible to map the electric potential and then the field $\underline{E}$. The flow lines are also easily computed, because of (6.8) which implies $\underline{v}$ to be perpendicular to either magnetic or electric fields

$$(6.11) \qquad \underline{v}\cdot\nabla\Phi = \underline{v}_\circ\,\underline{\nabla}\Psi = 0$$

So the streamlines are such that Ψ (magnetic potential) and Φ (electric potential) are constant.

In the case $B_\circ<0$ (i.e. in the so called "Dungey's case")

$$(6.12) \qquad \Phi = -v_\circ(2aB_\circ)^{1/2}(-\alpha)^{1/2}\,\mathrm{sen}(\beta/a)$$

Looking at the polar cap, where r=a the main contribution from the field comes from the dipole so that $\alpha = -a B_e\,\mathrm{sen}^2\vartheta$ and

$$(6.13) \qquad \Phi = -v_\circ(2B_\circ B_e)^{1/2}\, y$$

which means $\underline{E}=\underline{\text{const}}$ in the y direction (dawn to dusk).

In such way one can estimate potential differences from dawn to dusk as large as several 10^5 volts. This field across the polar cap means that an electric current flows across the polar ionosphere; this current penetrates into the dawn boundary of the polar cap along field lines then flowing upwards from the dusk boundary. These current sheets have actually been observed. In some intuitive way we can think of a sort of dynamo exciting a current system which flows in a stationary medium (the polar cup) and a moving medium across the magnetic field lines configuration. The model outlined above is very rough since the picture is much too semplicistic, but still valid to understand the basic physics.

Looking at the physical situation we can give some quantitative description of the current circulation: as a consequence of (6.8) the drift velocity $\underline{v}$ is to follow equipotential surfaces. On polar caps an ion moves in the direction of the x axis defining a constant potential, because of Φ proportional to y). Close to the boundary corresponding to $\vartheta = \vartheta_0$ the electric field must be perturbed, but beyond it, i.e. for $\vartheta > \vartheta_0$ the ion must continue its motion on an equipotential surface so that a circulation pattern is established in the polar cap as qualitatively described in fig. 18. What more specifically happens is that particles sharing a given interplanetary line of force before reaching point N_1 where the line is cut and reconnection takes place become separated beyond N_1 then moving as indicated above over the northern (or respectively southern) polar cap; at the boundary of the polar cap the two halves of field lines become again a single field line and particles start a return sunward motion.

6.2 The case of asymmetric models

It is quite clear that the symmetric field models considered above are not physically realistic (as also shown on the other hand from the very beginning by observations). Any even simple analytical treatment of asymmetries becomes impossible and only numerical methods can be used. So, before concluding, we shall look, at least qualitatively, to what the real situation of particle penetration into the magnetosphere is. The solar wind particles individual velocities and the field configuration are not in the real case as considered by simple models: a scatter of velocity either in value or in direction does exist and the field vector also is not uniform and or homoge-

neous. So the surface resembling the magnetopause is not a perfect barrier to the particle motion: some particles under favorable condition can go through it with a velocity component along the newly merged field lines close to the neutral point N_1 and drift toward the ionosphere. When individual velocities are very nearly aligned along the magnetic field lines they can penetrate deep enough to reach the ionosphere. On the other hand, ionospheric particles can escape from the ionosphere along the field lines. Favorable conditions for these two special kinds of drift happen in two northern and southern symmetrical regions shaped as a carved funnel of a tornado: they are called polar cusps (fig. 19). The very fact that the field is not always exactly (or even nearly) southward implies that some asymmetry between hemisphere can be expected because of the simultaneous conditions that $v_{\parallel}$ is unchanged, but the other component $\underline{v}$ is opposite in orientation when the interplanetary field is opposite (toward or away from the Sun). It is also clear that, beyond the polar cusps magnetic field lines are pushed antisunward giving origin to the so-called high latitude (or tail) lobe.

7. Conclusions. This short series of lectures was meant to give the audience the basic ideas constituting the background to understand general properties of the magnetospheric environment. Details are to be found in the references given below and in the original papers they refer to.

General references
Textbooks

Magneto-fluid mechanics II edition
by Ferraro and Plumpton
Clarendon Press, Oxford 1966

Dynamics of Geomagnetically Trapped Radiation,
by J.G. Roederer, Springer-Verlag, 1970

Earth's Magnetosphere.
by J.G. Roederer in "Solar System
Plasma Physics vol. 2, 1979

The Upper Atmosphere and Solar-Terrestrial
Relations
by J.K. Hargreaves, Van Nostrand 1979

Some specific or special references

Fairfield D.H., Electric and Magnetic Fields in
the High-latitude Magnetosphere
Rev. Geophys. Space Phys. 15, 285, 1977

Stern D.P., Large Scale Electric Fields in the
Earth's Magnetosphere
Rev. Geophys. Space Phys. 15, 156, 1977

Johnson F.S., The driving force for magnetospheric
Convection
Rev. Geophys. Space Phys. 16, 161, 1978

Stern D.P., An introduction to Magnetospheric
Physics by means of Simple Models
NASA Technical Memorandum 82072,
(contains workable exercises) January 1981

Spreiter J.R., A.L. Summers and A.Y. Alksne
Hydromagnetic flow around the magnetosphere
Planet. Space Science 14, 223, 1966

41 50

A description of instruments of use for magnetospheric physics is given on a special issue of IEEE Transactions on Geoscience and Electronics vol. GE-16 n.3 July 1978

A review on magnetometers ~~can be~~ for ~~[illegible]~~ space research is due to

N.F. Ness, Magnetometers for space research Space Science Rev. 11, 459, 1970

12 THE NATURE OF MAGNETIC FIELDS

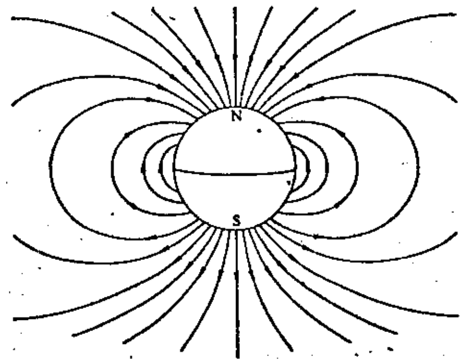

FIG. 2.1. Map of the lines of force of a dipole field such as the external magnetic field of earth. The arrows on the lines of force indicate the direction pointed by the north-seeking pole of a compass needle. The closed circle represents the surface of Earth with geographic north and south indicated at the top and bottom, respectively.

Earth's dipole field

Fig. 1

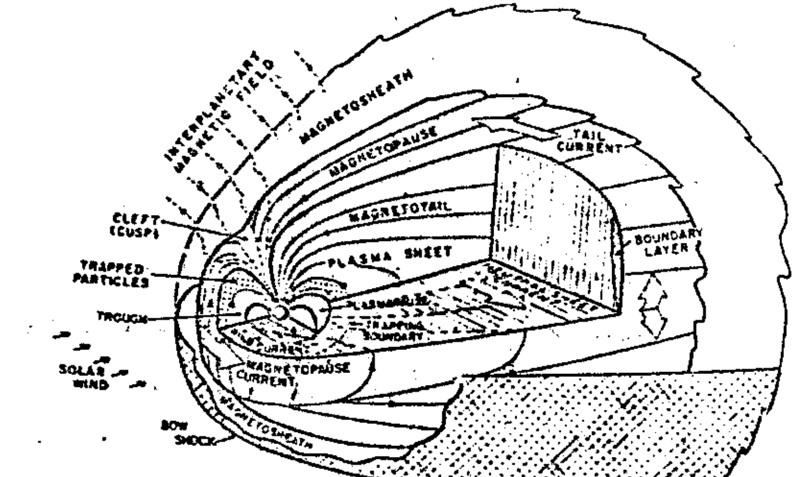

Fig. 1. A recent representation of the earth's magnetosphere, showing the numerous plasma regions which respond to solar wind changes and in turn interact with the ionosphere and atmosphere (courtesy of W. J. Heikkila, University of Texas).

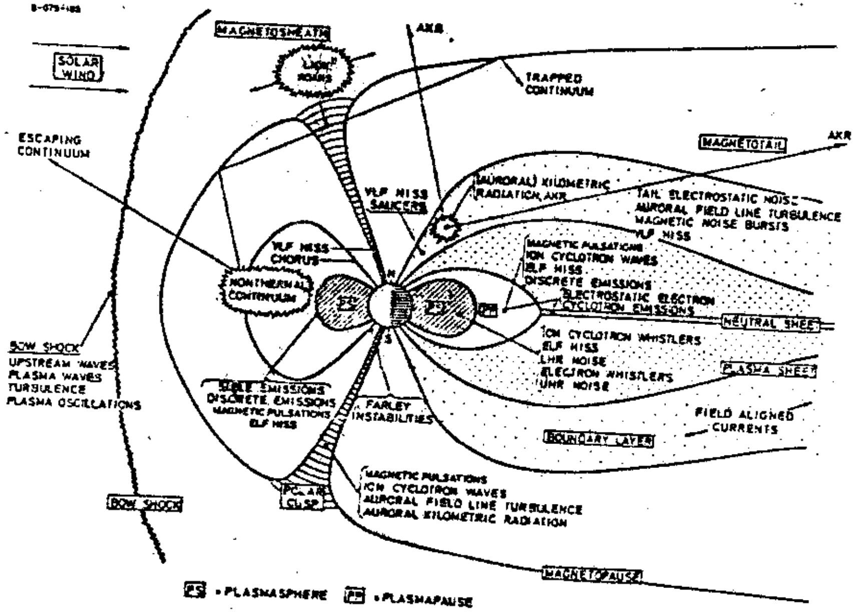

Fig 2

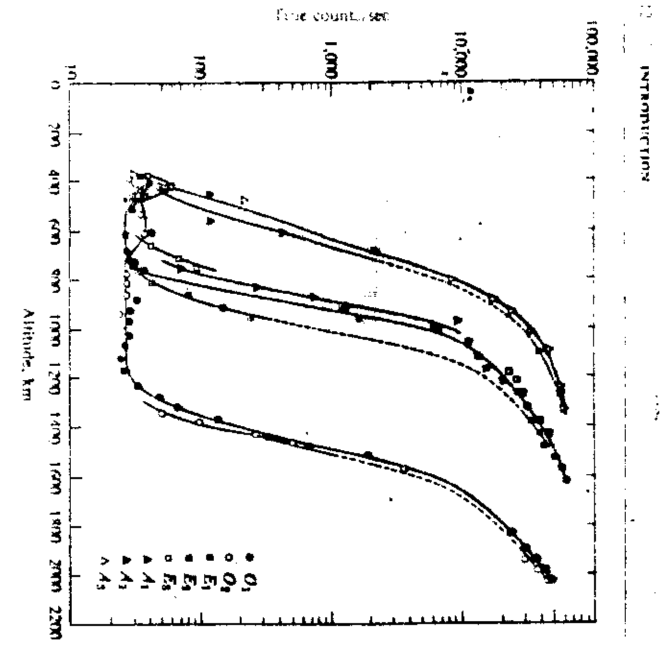

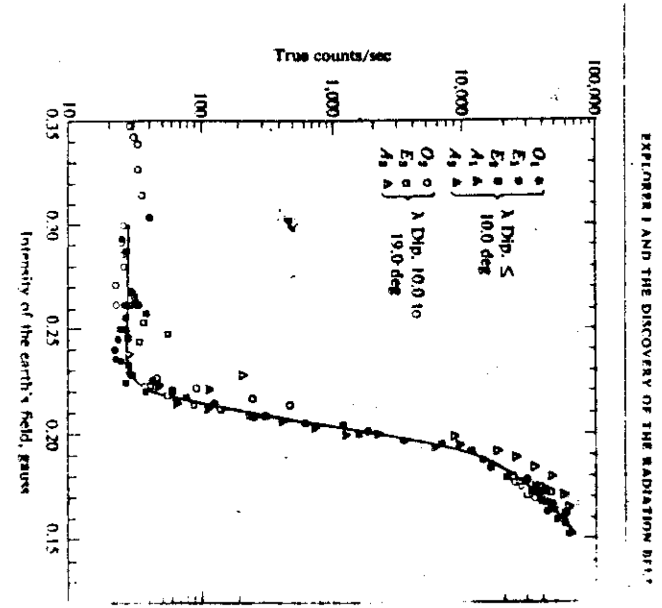

Fig 3

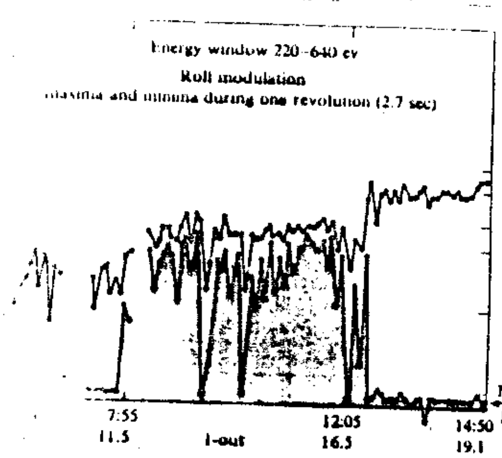

.39 Results from the MIT plasma probe showing measurements ...thermalized plasma by IMP I during outbound orbit 1. The posi- ... the boundaries are evidenced by the distinct spin modulation ...3 and 16.8R_E [137].

...milar solar-wind measurements made on the Vela satel- ...in the interplanetary medium is nearly monoenergetic and ...the magnetosheath the plasma is substantially thermalized, ...in energies, and is also roughly isotropic. This is what is ...es in plasma character as it crosses the shock front. ...analyzer plasma probe [139] on IMP I gave rather ...shock. It also saw the change in isotropy of the plasma at ...ge in energy spread. ...the data from the Ames plasma probe, has used the ...nguish the three regions of the space environment.

... Defined as corresponding to the appearance ...

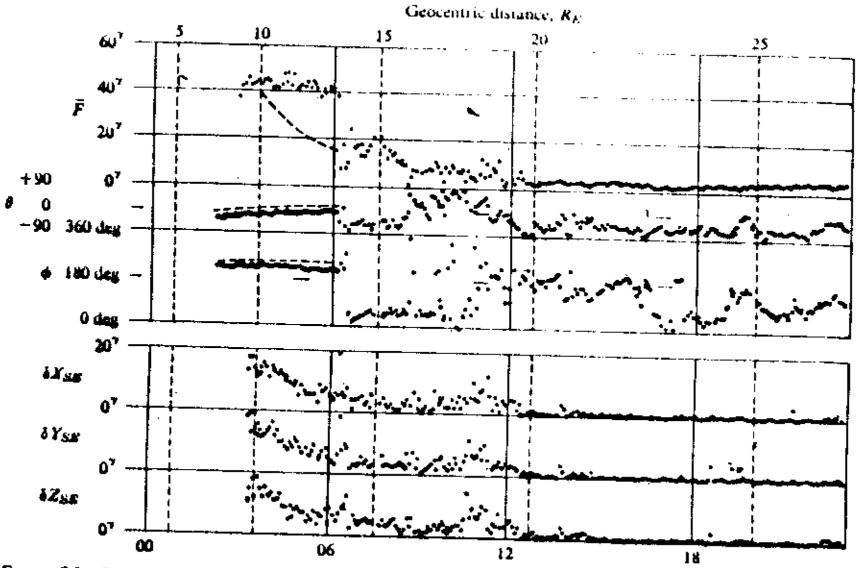

FIGURE 7.8 Geomagnetic field measurements on outbound orbit 11 from the IMP 1 satellite on January 5, 1964. The magnetosphere boundary is observed at a distance of 13.6R_E, and the shock wave at a distance of 19.7R_E. The satellite at this time was approximately on the sunrise terminator position with respect to the Earth-Sun line [24].

53

Fig 4

54

(a)

(b)

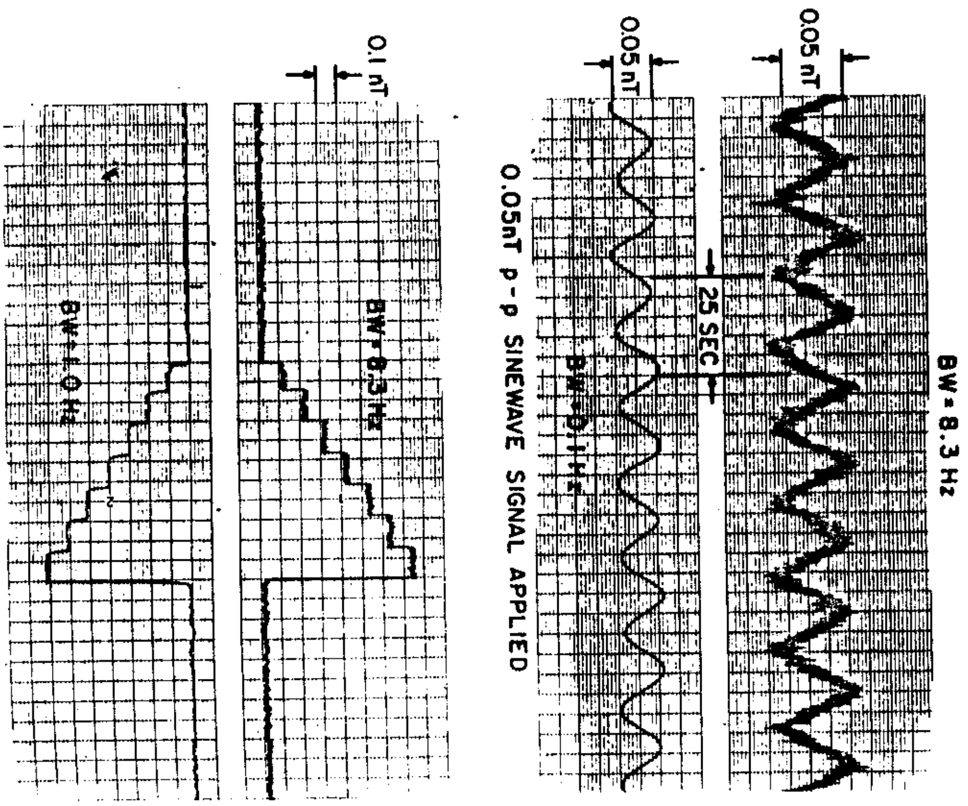

OPEN PROTOTYPE SENSOR

FIGURE 3

Fig 5

Fig. 6

55

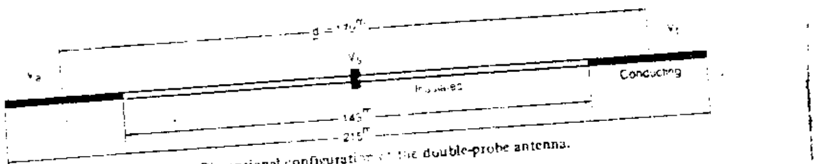

Fig. 1. Dimensional configuration of the double-probe antenna.

accompany transients in the dc field but associated in the plasma which would reflect either ...

The active elements, a and b, are 36-m uninsulated tip sec of two wires independently deployed to lengths of 106.

i experiment on the
nstrument measures
ectric fields with a
ures and diagnostic
nstrument operation

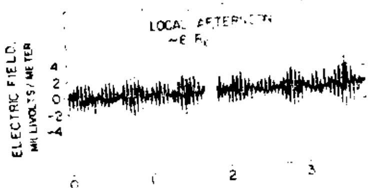

Fig. 1. The measured electric field as a function of time during a micropulsation event inside the magnetosphere

itential difference
ous carbon spheres
ooms and are sep-
SEE-1 satellite in

dynamic range of

ow 1000 Hz with
frequencies; and

o has a frequency
eed by the higher
ecraft. The con-
o used as a trans-

is two-dimensional
d magnitude of the
nt of the electric
nade in regions of
electric-field com-
assumed to be the
ectric field can be
mponents and this

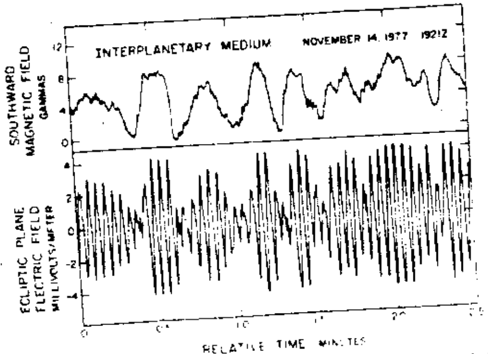

Fig. 2. The measured ecliptic plane component of the solar wind electric field and the component of magnetic field perpendicular to the ecliptic plane

field
mak
sphe
gain
peri
shor
exis
man
mag
far-
field
map
that
be i
be n
In
field
dens
exte
field
liabl
ment
the
craft
cont
perf
paras
adju
cont
proc
and
cess

56

TABELLA I

	MINIMO	MASSIMO	MEDIA
Velocità (km/sec)	200	800	400 ÷ 500
Densità n (ioni/cm³)	0.4	100	5
Temperatura T (K)	$5 \cdot 10^3$	10^6	$2 \cdot 10^5$
Abbondanza di elio (%) (rispetto ai protoni)	0	25	5
Flusso (particelle/cm²/sec)	10^8	10^{10}	$2 \div 3 \cdot 10^8$
Densità di energia, nkT (erg/cm³)	$8 \cdot 10^{-13}$	$3 \cdot 10^{-8}$	$3 \cdot 10^{-10}$

Fig 7

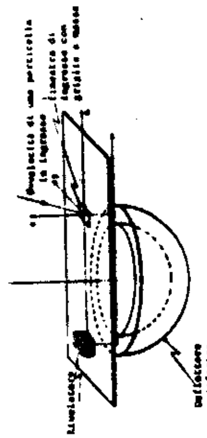

Fig. 2 - Schema di deflettore emisferico.

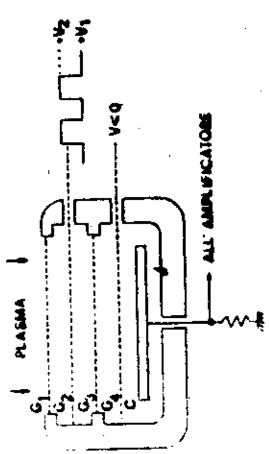

Fig. 1 - Schema di pozzo di Faraday. Le tensioni sono tutte riferite al corpo del satellite preso a potenziale zero.

Fig. 8

duplicate 57

58

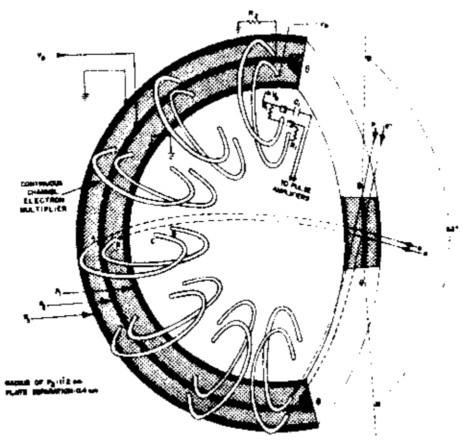

Fig. 8 Analyzer geometry and detector locations for the quadrispherical LEPEDEA.

(ISEE mission)

P_3 are tied to circuit ground and the center plate P_2 is supplied with a variable positive potential V_p which ranges from 0.08 V to 2.4 kV. This geometry of the electrostatic analyzer was chosen primarily because of its compactness and mechanical simplicity, i.e., only one curved plate with high voltage is required for two electrostatic analyzers, suitable energy passbands and geometry factors, and ability to provide angular distributions within a fan-shaped solid angle of view via the introduction of multiple detectors. The dimensions of the fan-shaped field-of-view are 6° X 162°. Positive ions and electrons entering the electrostatic analyzer at a given angle of incidence with respect to the plane of the entrance aperture will arrive at the exit aperture of the analyzer at a position determined by this angle of incidence (see particle paths in Fig. 1). Hence, by placing seven pairs of detectors at the

entire energy range is covered by 64 contigu The geometry factors for the positive ion chan mately 1.0×10^{-3} cm² sr. Geometry factors channels range from 1.5×10^{-4} cm² sr (pol 7.0×10^{-4} cm² sr (equatorial detectors). La tions were used to establish the geometry fact tron multiplier. The relative geometry facto in flight within isotropic plasmas. The sensitiv range of the instrument is sufficient for com surements of plasmas throughout the earth's and its environs, excluding only the solar win within the capabilities of the quadrispheric clude the dense convecting magnetoshea extremely tenuous regime of the magnetota hot diffuse ring current.

A thin-windowed GM tube with collimat of-view of full angle 40° is included with th mentation. This GM tube is sensitive to elect keV and protons with $E > 600$ keV. The fie monitor which is employed for survey mea energetic particle environment at the space directed perpendicular to the spin axis.

The electrical block diagram for the LEPEDEA is shown in Fig. 2. On the left figure are shown the fourteen electron mu GM tube with their associated high-voltage su fiers. Since the instrument has six high-vol analyzer-plate stepped voltage, four 3.8-kV the electron multipliers and a 700-V GM t considerable effort was expended in reduci possible one-point failures that would rend totally inoperable. Several of the important increase the reliability of the plasma analyze digital data system (DPU), dual low-voltag dual voltage step generators for the analyzer power switching for critical electronics syste ties of the instrument are extended by vario initiated by ground command and that are

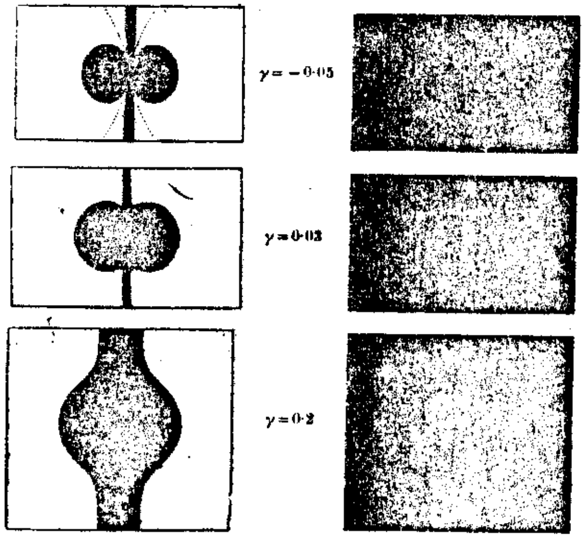

FIG. 28 (ii) Cases for different values of γ of the allowed spaces $Q\gamma$ (right row) and their sections by a meridian plane (in the row to the left, the allowed regions are white). The $q\gamma$ region is the right side of these sections.

Fig 10

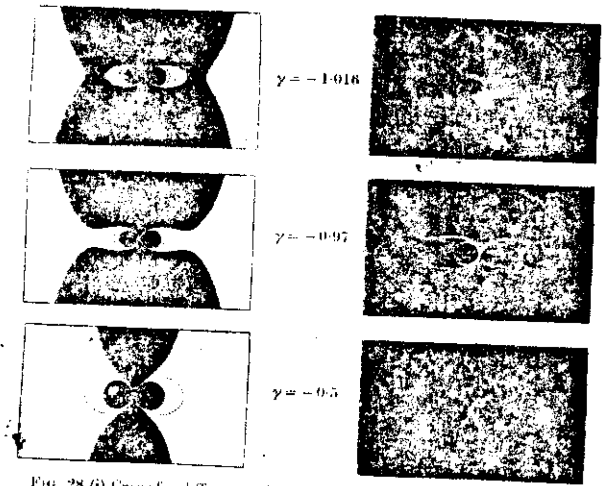

FIG. 28 (i) Cases for different values of γ of the allowed spaces $Q\gamma$ (right row) and their sections by a meridian plane (in the row to the left, the allowed regions are white). The $q\gamma$ region is the right side of these sections.

Fig 11

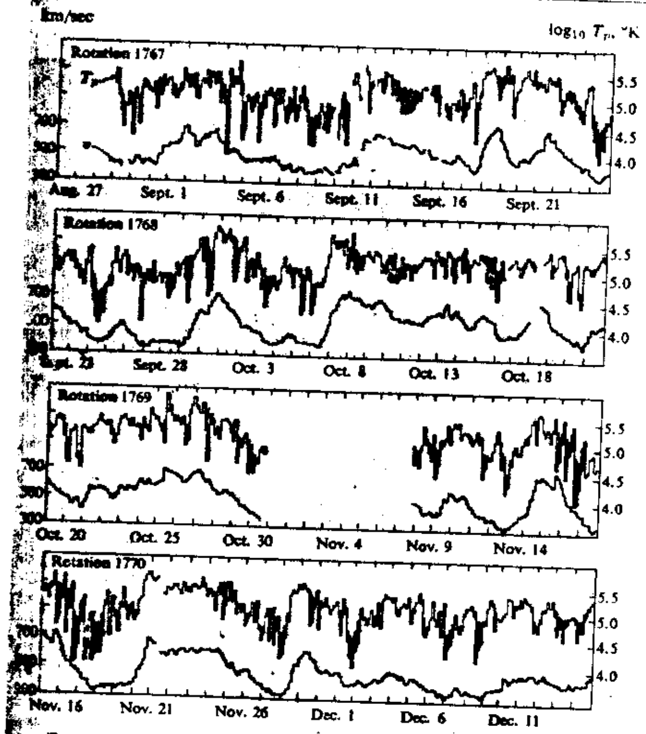

FIGURE 3.9 A comparison of the bulk velocity of the solar wind and the temperature of the solar wind on the Mariner flight [16].

ak flux of plasma of a particular velocity v appears at one particular ecliptic ngitude angle φ, and this angle changes with v. Partly this is due to the fact at particles of different energies have different observation angles but Wolfe owed the effect was more than this. To explain the observations he assumed at the velocity distribution function of the plasma in the frame of reference oving with the bulk velocity of the solar wind was a bi-Maxwellian given by

$$(v) = \exp\left(\frac{-mv_{\parallel}^2}{2KT_{\parallel}}\right) \exp\left(\frac{-mv_{\perp}^2}{2KT_{\perp}}\right) \qquad (3.14a)$$

Fig 12

61

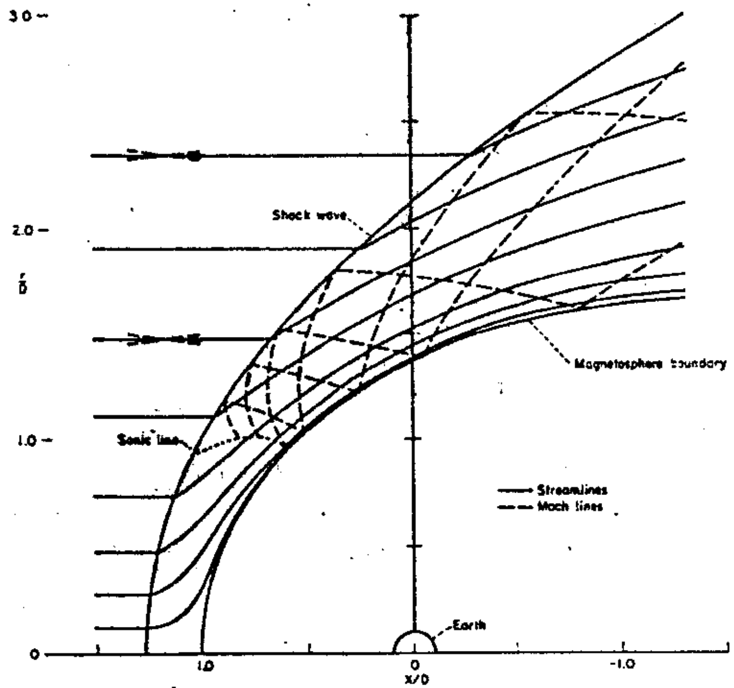

FIG. 9. STREAMLINES AND WAVE PATTERNS FOR SUPERSONIC FLOW PAST THE MAGNETOSPHERE; $M_\infty = 8, \gamma = \frac{5}{3}$.

without effect. This lack of dependence on Mach number does not apply, however, far downstream of the Earth where the bow wave approaches alignment with the asymptotic direction of weak discontinuities in the undisturbed incident solar wind. The variation of density, velocity and mass flux along the magnetosphere boundary and the downstream side of the shock wave are shown in Fig. 14. The most striking conclusion is that these quantities are virtually independent of Mach number, and only slightly dependent on γ. On the other hand, results presented in Fig. 15 show that the temperature depends strongly on Mach number and γ, with higher values associated with higher Mach numbers and larger γ, a trend clearly revealed by inspection of equation (28).

A useful quantity for characterizing the location of the bow shock wave is the standoff distance Δ at the nose of the magnetosphere. This distance is controlled to a large degree by mass conservation considerations, since the mass flow passing between the magnetosphere and the bow wave at any station must match that crossing the bow wave inside that station. More specifically, the standoff distance at high Mach numbers is determined almost entirely

Fig 13

62

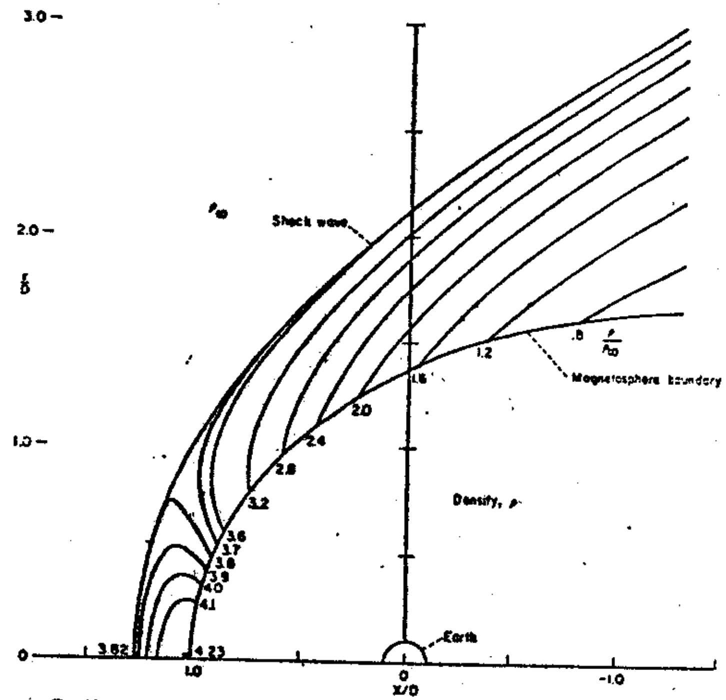

FIG. 10. DENSITY CONTOURS FOR SUPERSONIC FLOW PAST THE MAGNETOSPHERE; $M_\infty = 8, \gamma = \frac{5}{3}$.

by the density ratio ρ_1/ρ_∞ across the bow wave on the stagnation streamline. The latter is related to the free-stream Mach number and the ratio of specific heats according to the following expression:

$$\frac{\rho_1}{\rho_\infty} = \frac{(\gamma + 1)M_\infty^2}{(\gamma - 1)M_\infty^2 + 2} \tag{29}$$

The variation of standoff distance with ρ_1/ρ_∞ is presented for a wide range of values for γ and free-stream Mach number M_∞ in Fig. 16. As previously shown in an aerodynamic context by Seiff[34] and Inouye,[35] this distance varies nearly linearly with ρ_∞/ρ_1 over a wide range of conditions. With the standoff distance Δ normalized by the distance D from the center of the Earth to the nose of the magnetosphere, the following simple empirical formula emerges

$$\Delta/D = 1{\cdot}1\rho_\infty/\rho_1 \tag{30}$$

In order to illustrate further details of supersonic flow of a compressible gas past the magnetosphere, an experiment was conducted in the Ames Research Center, Supersonic

Fig 14

63

64

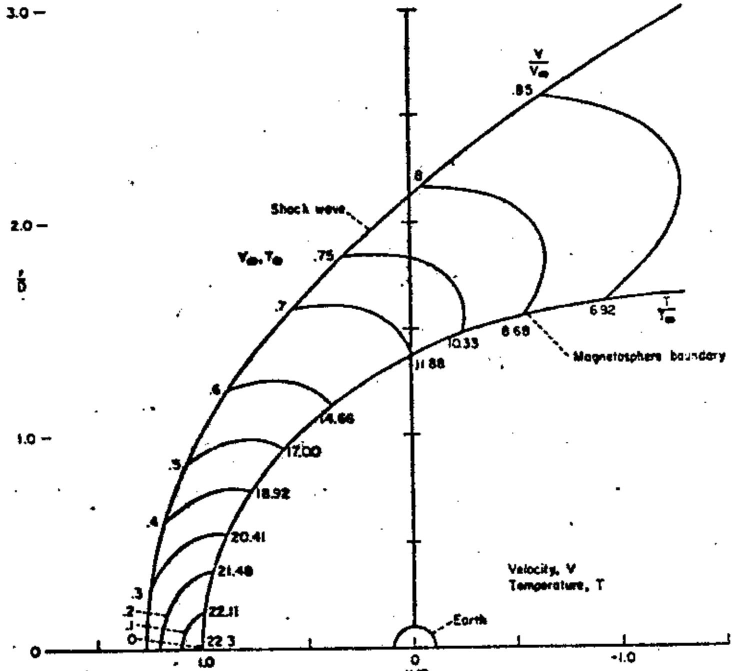

FIG. 11. VELOCITY AND TEMPERATURE CONTOURS FOR SUPERSONIC FLOW PAST THE MAGNETOSPHERE; $M_\infty = 8$, $\gamma = \frac{5}{3}$.

Free Flight Wind Tunnel, by Donn Kirk in which shadowgraph photographs were taken of a metal model of the magnetosphere in flight at Mach numbers between about 4·5 and 5 through argon. In normal use of this facility, models are fired from a 50 caliber light-gas gun upstream through an elongated test section of an otherwise normal supersonic wind tunnel. The working fluid normally employed is air, but other gases can be used for a more limited range of test conditions that can be reached by shooting the models into stationary gas. In other words, the wind tunnel is only used as a tank to contain the gas into which the model is fired as in a conventional ballistics range. Since the relative velocity between any given projectile and the gas is thus limited by the allowable muzzle velocity, the maximum Mach number that can be attained depends primarily on the speed of sound in the gas in the test section. By selecting argon as the gas, it is possible to obtain a value of $\frac{5}{3}$ for γ and a low enough speed of sound that Mach numbers as high as 4·5 or 5 can be achieved by firing the projectile into stationary gas. Although these conditions are not identical with those

Fig 15

Fig 16

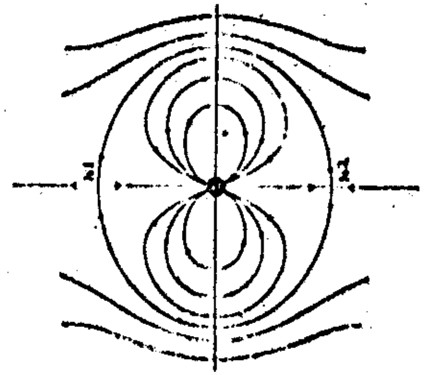

Figure 8

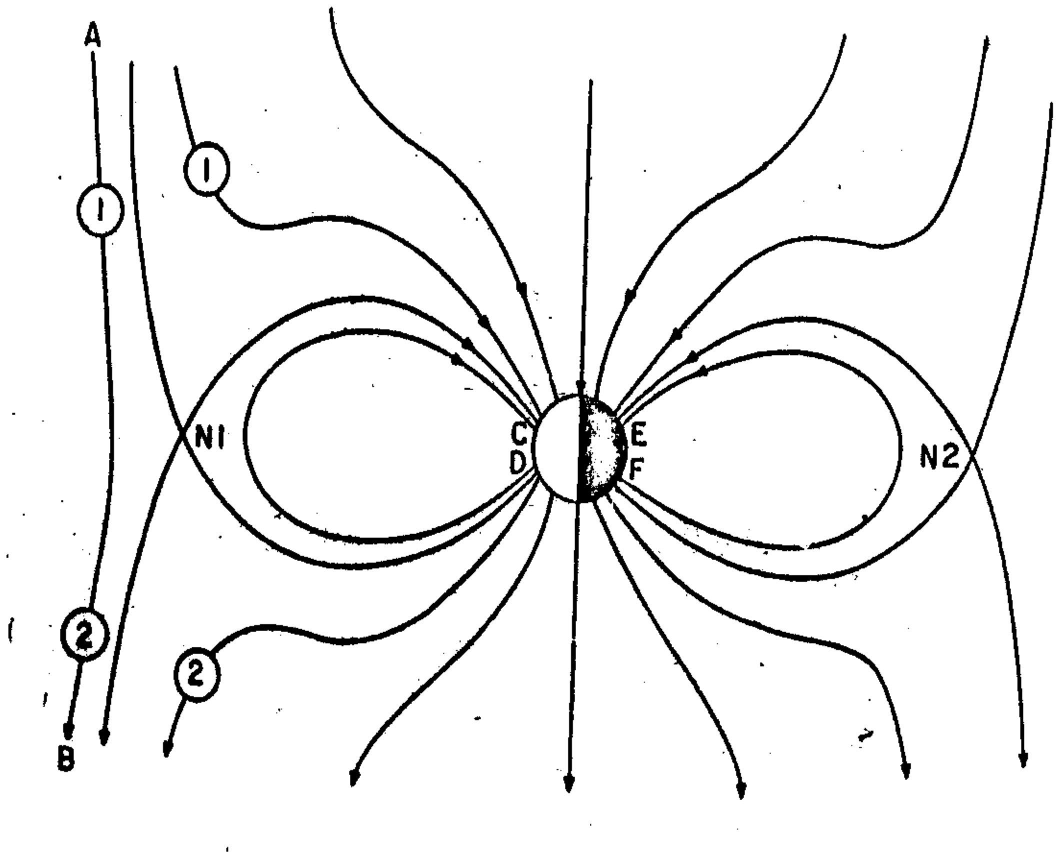

Figure #

Fig 17

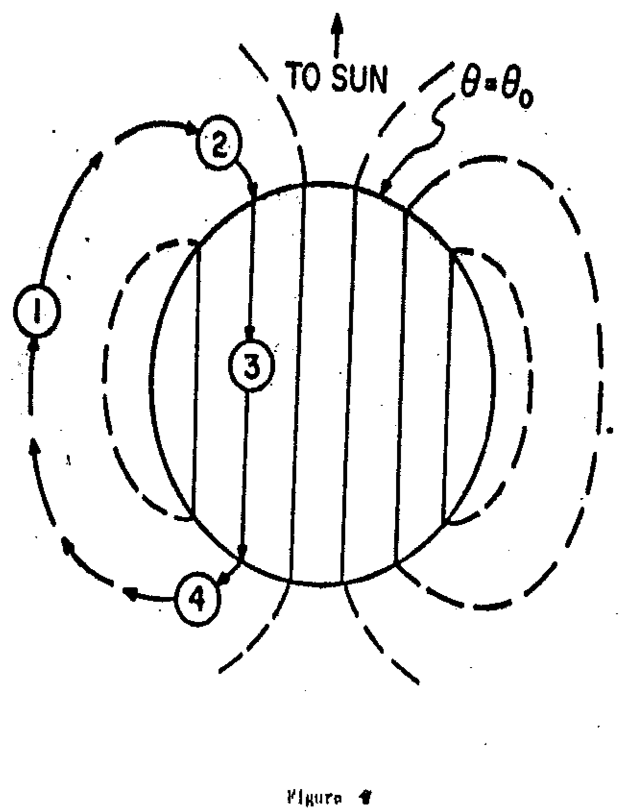

Figure #

Fig 18

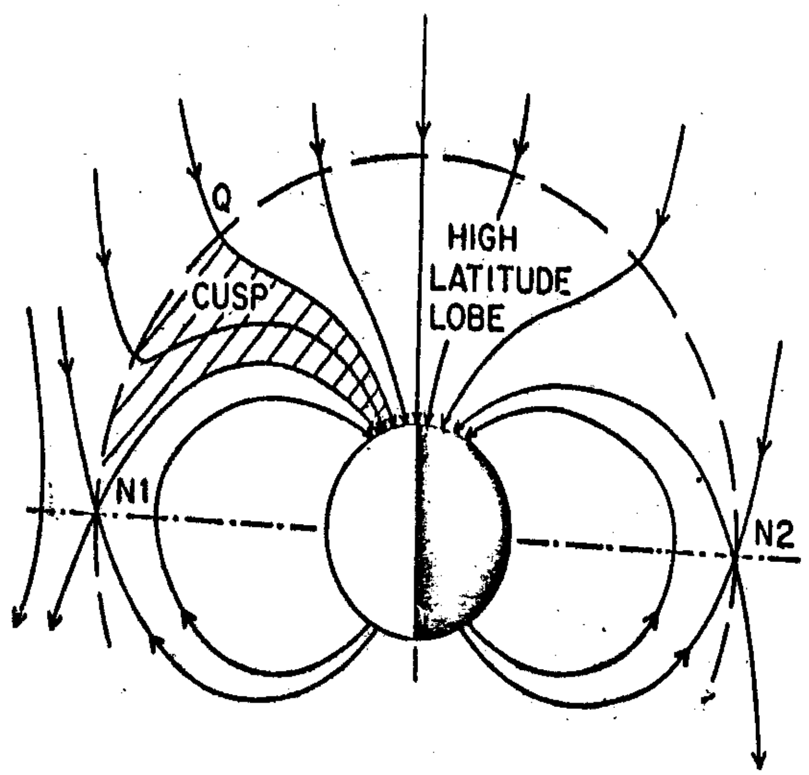

Figure 4

Fig 19